high metastatic potential. In contrast, HSC4 cells show low metastatic potential. No metastatic sublines are derived from HSC4 cells [90]. Metastatic HSC3 cells show colony formation in type I collagen matrix, adherence to type IV collagen [90], high heparanase activity [91], and reduced nm23H1 expression and upregulated MMP-2 and -9 [92] in comparison with HSC4 cells. HSC3 cells show overexpression of MIA, HMGB1, NFkBp65, VEGF-C, and VEGF-D in comparison with HSC4 cells [61]. Thus, the increase of lymphangiogenic capacity might be associated with high potential of lymph nodes metastasis in HSC3. The lymphangiogenic capacity is needed to further examination to control lymph node metastasis in OSCCs. MIA-expression associated with a high incidence of lymph node metastasis, whereas MIA-expression did not correlate with recurrence or with disease-free survival. RAGE–HMGB1 co-expression is associated with T classification (extension of primary tumor) but not nodal metastasis in OSCCs; however, RAGE expression is closely associated with recurrence and disease-free survival [52, 53, 93]. In this context, other RAGE agonists such as AGE, S100, amyloid proteins should be examined the angiogenic capacity.

Many OSCCs recur at the local sites but not from nodal metastasis. Local recurrence of OSCC depends on aggressiveness of cancer invasion and anatomical difficulties in the head to obtain sufficient surgical margins. In OSCC, both metastatic potential and local aggressiveness are significant factors to determine the disease outcome.

Future perspectives

We clarified that extracellular HMGB1–RAGE signal induces angiogenesis, and intracellular HMGB1–MIA system accelerates lymphangiogenesis in OSCC. However, the detailed mechanism of HMGB1–RAGE and HMGB1–MIA related angiogenesis and lymphangiogenesis, respectively. In comparison with normal vessels, tumoral irregular vessels are irregular and attenuated for delivery of anti-cancer drug [94]. Recently, it has been proposed normalization of tumoral vessels are easy to effect anti-cancer therapy [95, 96]. Inhibition of HMGB1 signals might be useful target of normalization of tumoral vessels. An appropriate animal experiment will be needed in further examination and we must confirm whether HMGB1 related signal is useful target for anti-angiogenic and anti-lymphangiogenic therapy in OSCC.

Conclusion

As shown in Fig. 2, a scheme is proposed that overexpressed HMGB1 activates RAGE to induce angiogenesis as a cytokines, which is associated with local progression of OSCCs. HMGB1 also enhances MIA expression to induce lymphangiogenesis as a transcriptional co-factor, which is associated with lymph node metastasis. Therefore, HMGB1 plays a pivotal role in aggressiveness of OSCC. HMGB1 might be a good marker for malignant potential of OSCC and be a potent target for therapeutics of OSCC.

Conflict of interest None.

References

1. Paterson IC, Eveson JW, Prime SS (1996) Molecular changes in oral cancer may reflect and ethnic origin. Eur J Cancer B Oral Oncol 32B:150–153
2. Kaura J, Srivastava A, Ralhan R (1994) Overexpression of p53 protein in betel-and tobacco-related human oral dysplasia and squamous-cell carcinoma in India. Int J Cancer 58:340–345
3. Chen YJ, Lin SC, Kao T et al (2004) Genome-wide profiling of oral squamous cell carcinoma. J Pathol 204:326–332
4. Hunter KD, Parkinson EK, Harrison PR (2005) Profiling early head and neck cancer. Nat Rev Cancer 5:127–135
5. Tanaka S, Sobue T (2005) Comparison of oral and pharyngeal cancer mortality in five countries: France, Italy, Japan, UK and USA from the WHO Mortality Database (1960–2000). Jpn J Clin Oncol 35:488–491
6. Nagler RM (2002) Molecular aspects of oral cancer. Anticancer Res 22:2977–2980
7. Lopez-Graniel CM, Tamez de Leon D, Meneses-Garcia A et al (2001) Tumor angiogenesis as a prognostic factor in oral cavity carcinomas. J Exp Clin Cancer Res 20:463–468
8. Lippman SM, Hong WK (2001) Molecular markers of the risk of oral cancer. N Engl J Med 344:1323–1326
9. Hershkovich O, Oliva J, Nagler RM (2004) Lethal synergistic effect of cigarette smoke and saliva in an in vitro model: does saliva have a role in the development of oral cancer? Eur J Cancer 40:1760–1767
10. Vokes EE, Weichselbaum RR, Lippman SM et al (1993) Head and neck cancer. N Engl J Med 328:189–194
11. Alvi A, Johnson JT (1997) Development of distant metastasis after treatment of advanced-stage head and neck cancer. Head Neck 19:500–505
12. Sawair FA, Irwin CR, Gordon DJ et al (2003) Invasive front grading: reliability and usefulness in the management of oral squamous cell carcinoma. J Oral Pathol Med 32:1–9
13. Schliephake H (2003) Prognostic relevance of molecular markers of oral cancer–a review. Int J Oral Maxillofac Surg 32:233–245
14. Alcalde RE, Terakado N, Otsuki K et al (1997) Angiogenesis and expression of platelet-derived endothelial cell growth factor in oral squamous cell carcinoma. Oncology 54:324–328
15. Li C, Shintani S, Terakado N et al (2005) Microvessel density and expression of vascular endothelial growth factor, basic fibroblast growth factor, and platelet-derived endothelial growth factor in oral squamous cell carcinomas. Int J Oral Maxillofac Surg 34:559–565
16. Shang ZJ, Li ZB, Li JR (2006) VEGF is up-regulated by hypoxic stimulation and related to tumour angiogenesis and severity of disease in oral squamous cell carcinoma: in vitro and in vivo studies. Int J Oral Maxillofac Surg 35:533–538
17. Watanabe H, Iwase M, Ohashi M et al (2002) Role of interleukin-8 secreted from human oral squamous cell carcinoma cell lines. Oral Oncol 38:670–679

18. Kuniyasu H, Oue N, Wakikawa A et al (2002) Expression of receptors for advanced glycation end-products (RAGE) is closely associated with the invasive and metastatic activity of gastric cancer. J Pathol 196:163–170
19. Kuniyasu H, Chihara Y, Kondo H et al (2003) Amphoterin induction in prostatic stromal cells by androgen deprivation is associated with metastatic prostate cancer. Oncol Rep 10:1863–1868
20. Kuniyasu H, Chihara Y, Kondo H (2003) Differential effects between amphoterin and advanced glycation end products on colon cancer cells. Int J Cancer 104:722–727
21. Kuniyasu H, Chihara Y, Takahashi T (2003) Co-expression of receptor for advanced glycation end products and the ligand amphoterin associates closely with metastasis of colorectal cancer. Oncol Rep 10:445–448
22. Goodwin GH, Sanders C, Johns EW (1973) A new group of chromatin-associated proteins with a high content of acidic and basic amino acids. Eur J Biochem 38:14–19
23. Pasheva EA, Ugrinova I, Spassovska N et al (2002) The binding affinity of HMG1 protein to DNA modified by cis-platin and its analogs correlates with their antitumor activity. Int J Biochem Cell Biol 34:87–92
24. Stros M, Ozaki T, Bacikova A et al (2002) HMGB1 and HMGB2 cell-specifically down-regulate the p53- and p73-dependent sequence-specific transactivation from the human Bax gene promoter. J Biol Chem 277:7157–7164
25. Ugrinova I, Pasheva EA, Armengaud J et al (2001) In vivo acetylation of HMG1 protein enhances its binding affinity to distorted DNA structures. Biochemistry 40:14655–14660
26. Calogero S, Grassi F, Aguzzi A et al (1999) The lack of chromosomal protein Hmg1 does not disrupt cell growth but causes lethal hypoglycaemia in newborn mice. Nat Genet 22:276–280
27. Huttunen HJ, Kuja-Panula J, Sorci G et al (2000) Coregulation of neurite outgrowth and cell survival by Amphoterin and S100 proteins through receptor for advanced glycation end products (RAGE) activation. J Biol Chem 275:40096–40105
28. Parkkinen J, Raulo E, Merenmies J et al (1993) Amphoterin, the 30-kDa protein in a family of HMG1-type polypeptides. Enhanced expression in transformed cells, leading edge localization, and interactions with plasminogen activation. J Biol Chem 268:19726–19738
29. Andersson U, Erlandsson-Harris H, Yang H et al (2002) HMGB1 as a DNA-binding cytokine. J Leukoc Biol 72:1084–1091
30. Kim JY, Park JS, Strassheim D et al (2005) HMGB1 contributes to the development of acute lung injury after hemorrhage. Am J Physiol Lung Cell Mol Physiol 288:L958–L965
31. Yang H, Wang H, Czura CJ et al (2002) HMGB1 as a cytokine and therapeutic target. J Endotoxin Res 8:469–472
32. Yang H, Wang H, Tracey KJ (2001) HMG-1 rediscovered as a cytokine. Shock 15:247–253
33. Tang D, Shi Y, Jang L et al (2005) Heat shock response inhibits release of high mobility group box 1 protein induced by endotoxin in murine macrophages. Shock 23:434–440
34. Watanabe T, Kubota S, Nagaya M et al (2005) The role of HMGB-1 on the development of necrosis during hepatic ischemia and hepatic ischemia/reperfusion injury in mice. J Surg Res 124:59–66
35. Andersson U, Erlandsson-Harris H (2004) HMGB1 is a potent trigger of arthritis. J Intern Med 255:344–350
36. Huttunen HJ, Rauvala H (2004) Amphoterin as an extracellular regulator of cell motility: from discovery to disease. J Intern Med 255:351–366
37. Wang H, Yang H, Tracey KJ (2004) Extracellular role of HMGB1 in inflammation and sepsis. J Intern Med 255:320–331
38. Czura CJ, Wang H, Tracey KJ (2001) Dual roles for HMGB1: DNA binding and cytokine. J Endotoxin Res 7:315–321
39. Gardella S, Andrei C, Ferrera D et al (2002) The nuclear protein HMGB1 is secreted by monocytes via a non-classical, vesicle-mediated secretory pathway. EMBO Rep 3:995–1001
40. Bonaldi T, Talamo F, Scaffidi P et al (2003) Monocytic cells hyperacetylate chromatin protein HMGB1 to redirect it towards secretion. EMBO J 22:551–5560
41. Fujii K, Luo Y, Sasahira T et al (2009) Co-treatment with deoxycholic acid and azoxymethane accelerates the secretion of HMGB1 in IEC6 intestinal epithelial cells. Cell Prolif 42:701–709
42. Scaffidi P, Misteli T, Bianchi ME (2002) Release of chromatin protein HMGB1 by necrotic cells triggers inflammation. Nature 418:191–195
43. Lalla E, Lamster IB, Schmidt AM (1998) Enhanced interaction of advanced glycation end products with their cellular receptor RAGE: implications for the pathogenesis of accelerated periodontal disease in diabetes. Ann Periodontol 3:13–19
44. Schmidt AM, Hofmann M, Taguchi A et al (2000) RAGE: a multiligand receptor contributing to the cellular response in diabetic vasculopathy and inflammation. Semin Thromb Hemost 26:485–493
45. Schmidt AM, Stern DM (2000) RAGE: a new target for the prevention and treatment of the vascular and inflammatory complications of diabetes. Trends Endocrinol Metab 11:368–375
46. Rauvala H, Huttunen HJ, Fages C et al (2000) Heparin-binding proteins HB-GAM (pleiotrophin) and amphoterin in the regulation of cell motility. Matrix Biol 19:377–387
47. Taguchi A, Blood DC, del Toro G et al (2000) Blockade of RAGE-amphoterin signalling suppresses tumour growth and metastases. Nature 405:354–360
48. Kuniyasu H, Sasahira T, Sasaki T et al (2004) Depletion of infiltrating macrophages is associated with amphoterin expression in colon cancer. Pathobiology 71:129–136
49. Kuniyasu H, Yano S, Sasaki T et al (2005) Colon cancer cell-derived high mobility group 1/amphoterin induces growth inhibition and apoptosis in macrophages. Am J Pathol 166:751–760
50. Sasahira T, Sasaki T, Kuniyasu H et al (2005) Interleukin-15 and transforming growth factor alpha are associated with depletion of tumor-associated macrophages in colon cancer. J Exp Clin Cancer Res 24:69–74
51. Ishiguro H, Nakaigawa N, Miyoshi Y et al (2005) Receptor for advanced glycation end products (RAGE) and its ligand, amphoterin are overexpressed and associated with prostate cancer development. Prostate 64:92–100
52. Sasahira T, Kirita T, Bhawal UK et al (2007) The expression of receptor for advanced glycation end products is associated with angiogenesis in human oral squamous cell carcinoma. Virchows Arch 450:287–295
53. Sasahira T, Kirita T, Bhawal UK et al (2007) Receptor for advanced glycation end products (RAGE) is important in the prediction of recurrence in human oral squamous cell carcinoma. Histopathology 51:166–172
54. Yamamoto K, Kitayama W, Denda A et al (2006) Expression of receptor for advanced glycation end products during rat tongue carcinogenesis by 4-nitroquinoline 1-oxide and effect of a selective cyclooxygenase-2 inhibitor, etodolac. Pathobiology 73:317–324
55. Liu W, Ahmad SA, Reinmuth N et al (2000) Endothelial cell survival and apoptosis in the tumor vasculature. Apoptosis 5:323–328
56. Gasparini G, Harris AL (1995) Clinical importance of the determination of tumor angiogenesis in breast carcinoma: much more than a new prognostic tool. J Clin Oncol 13:765–782

57. Fidler IJ (1997) Critical determinants of human colon cancer metastasis. In: Tahara E (ed) Molecular pathology of gastroenterological cancer. Springer, Tokyo, pp 147–169
58. Hanahan D (1997) Signaling vascular morphogenesis and maintenance. Science 277:48–50
59. Nakazato T, Shingaki S, Kitamura N et al (2006) Expression level of vascular endothelial growth factor-C and -A in cultured human oral squamous cell carcinoma correlates respectively with lymphatic metastasis and angiogenesis when transplanted into nude mouse oral cavity. Oncol Rep 15:825–830
60. Shintani S, Li C, Ishikawa T et al (2004) Expression of vascular endothelial growth factor A, B, C, and D in oral squamous cell carcinoma. Oral Oncol 40:13–20
61. Sasahira T, Kirita T, Oue N et al (2008) High mobility group box-1-inducible melanoma inhibitory activity is associated with nodal metastasis and lymphangiogenesis in oral squamous cell carcinoma. Cancer Sci 99:1806–1812
62. Miyata Y, Kanda S, Ohba K et al (2006) Lymphangiogenesis and angiogenesis in bladder cancer: prognostic implications and regulation by vascular endothelial growth factors-A, -C, and -D. Clin Cancer Res 12:800–806
63. Joukov V, Pajusola K, Kaipainen A et al (1996) A novel vascular endothelial growth factor, VEGF-C, is a ligand for the Flt4 (VEGFR-3) and KDR (VEGFR-2) receptor tyrosine kinases. EMBO J 15:1751
64. Yamagishi S, Takeuchi M, Inagaki Y et al (2003) Role of advanced glycation end products (AGEs) and their receptor (RAGE) in the pathogenesis of diabetic microangiopathy. Int J Clin Pharmacol Res 23:129–134
65. Brownlee M (1995) Advanced protein glycosylation in diabetes and aging. Annu Rev Med 46:223–234
66. Yamamoto Y, Yamagishi S, Yonekura H et al (2000) Roles of the AGE-RAGE system in vascular injury in diabetes. Ann N Y Acad Sci 902:163–170 (discussion 170–162)
67. Okamoto T, Yamagishi S, Inagaki Y et al (2002) Angiogenesis induced by advanced glycation end products and its prevention by cerivastatin. FASEB J 16:1928–1930
68. Treins C, Giorgetti-Peraldi S, Murdaca J et al (2001) Regulation of vascular endothelial growth factor expression by advanced glycation end products. J Biol Chem 276:43836–43841
69. Tsai PW, Shiah SG, Lin MT et al (2003) Up-regulation of vascular endothelial growth factor C in breast cancer cells by heregulin-beta 1. A critical role of p38/nuclear factor-kappa B signaling pathway. J Biol Chem 278:5750–5759
70. Blesch A, Bosserhoff AK, Apfel R et al (1994) Cloning of a novel malignant melanoma-derived growth-regulatory protein, MIA. Cancer Res 54:5695–5701
71. Bosserhoff AK, Hein R, Bogdahn U et al (1996) Structure and promoter analysis of the gene encoding the human melanoma-inhibiting protein MIA. J Biol Chem 271:490–495
72. Koehler MR, Bosserhoff A, von Beust G et al (1996) Assignment of the human melanoma inhibitory activity gene (MIA) to 19q13.32–q13.33 by fluorescence in situ hybridization (FISH). Genomics 35:265–267
73. Bosserhoff AK, Moser M, Hein R et al (1999) In situ expression patterns of melanoma-inhibiting activity (MIA) in melanomas and breast cancers. J Pathol 187:446–454
74. Bosserhoff AK, Kaufmann M, Kaluza B et al (1997) Melanoma-inhibiting activity, a novel serum marker for progression of malignant melanoma. Cancer Res 57:3149–3153
75. Poser I, Tatzel J, Kuphal S et al (2004) Functional role of MIA in melanocytes and early development of melanoma. Oncogene 23:6115–6124
76. Bosserhoff AK, Kondo S, Moser M et al (1997) Mouse CD-RAP/MIA gene: structure, chromosomal localization, and expression in cartilage and chondrosarcoma. Dev Dyn 208:516–525
77. Hau P, Ruemmele P, Kunz-Schughart LA et al (2004) Expression levels of melanoma inhibitory activity correlate with time to progression in patients with high-grade glioma. Oncol Rep 12:1355–1364
78. El Fitori J, Kleeff J, Giese NA et al (2005) Melanoma Inhibitory Activity (MIA) increases the invasiveness of pancreatic cancer cells. Cancer Cell Int 5:3
79. Bosserhoff AK, Stoll R, Sleeman JP et al (2003) Active detachment involves inhibition of cell-matrix contacts of malignant melanoma cells by secretion of melanoma inhibitory activity. Lab Invest 83:1583–1594
80. Jachimczak P, Apfel R, Bosserhoff AK et al (2005) Inhibition of immunosuppressive effects of melanoma-inhibiting activity (MIA) by antisense techniques. Int J Cancer 113:88–92
81. Bauer R, Humphries M, Faessler R et al (2006) Regulation of integrin activity by MIA. J Biol Chem 281:11669–11677
82. Dietrich T, Onderka J, Bock F et al (2007) Inhibition of inflammatory lymphangiogenesis by integrin α5 blockade. Am J Pathol 171:361–372
83. Stacker SA, Achen MG, Jussila L et al (2002) Lymphangiogenesis and cancer metastasis. Nat Rev Cancer 2:573–583
84. O-charoenrat P, Rhys-Evans P, Eccles SA (2001) Expression of vascular endothelial growth factor family members in head and neck squamous cell carcinoma correlates with lymph node metastasis. Cancer 92:556–568
85. Stacker SA, Caesar C, Baldwin ME et al (2001) VEGF-D promotes the metastatic spread of tumor cells via the lymphatics. Nat Med 7:186–191
86. Xie K, Wei D, Shi Q et al (2004) Constitutive and inducible expression and regulation of vascular endothelial growth factor. Cytokine Growth Factor Rev 15:297–324
87. Kobayashi S, Kishimoto T, Kamata S et al (2007) Rapamycin, a specific inhibitor of the mammalian target of rapamycin, suppresses lymphangiogenesis and lymphatic metastasis. Cancer Sci 98:726–733
88. Poser I, Golob M, Buettner R et al (2003) Upregulation of HMG1 leads to melanoma inhibitory activity expression in malignant melanoma cells and contributes to their malignancy phenotype. Mol Cell Biol 23:2991–2998
89. Golob M, Buettner R, Bosserhoff AK (2000) Characterization of a transcription factor binding site, specifically activating MIA transcription in melanoma. J Invest Dermatol 115:42–47
90. Momose F, Araida T, Negishi A et al (1989) Variant sublines with different metastatic potentials selected in nude mice from human oral squamous cell carcinomas. J Oral Pathol Med 18:391–395
91. Ikuta M, Podyma KA, Maruyama K et al (2001) Expression of heparanase in oral cancer cell lines and oral cancer tissues. Oral Oncol 37:177–184
92. Khan MH, Yasuda M, Higashino F et al (2001) nm23-H1 suppresses invasion of oral squamous cell carcinoma-derived cell lines without modifying matrix metalloproteinase-2 and matrix metalloproteinase-9 expression. Am J Pathol 158:1785–1791
93. Bhawal UK, Ozaki Y, Nishimura M et al (2005) Association of expression of receptors for advanced glycation end-products (RAGE) and invasive and metastatic activity of oral squamous cell carcinoma. Oncology 69:246–255
94. Jain RK, Munn LL, Fukumura D (2002) Dissecting tumour pathophysiology using intravital microscopy. Nat Rev Cancer 2:266–276
95. Tong RT, Boucher Y, Kozin SV et al (2004) Vascular normalization by vascular endothelial growth factor receptor 2 blockade induces a pressure gradient across the vasculature and improves drug penetration in tumors. Cancer Res 64:3731–3736
96. Jain RK (2005) Normalization of tumor vasculature: an emerging concept in antiangiogenic therapy. Science 307:58–62

Biochemical and Biophysical Research Communications 406 (2011) 529–533

Contents lists available at ScienceDirect

Biochemical and Biophysical Research Communications

journal homepage: www.elsevier.com/locate/ybbrc

In vitro enhanced differentiation of neural networks in ES gut-like organ from mouse ES cells by a 5-HT_4-receptor activation

Miyako Takaki [a,*], Hiromi Misawa [a], Hiroko Matsuyoshi [a], Isao Kawahara [a], Kei Goto [a], Guo-Xing Zhang [a], Koji Obata [a], Hiroki Kuniyasu [b]

[a] Department of Physiology II, Nara Medical University, School of Medicine, Kashihara, Nara 634-8521, Japan
[b] Department of Molecular Pathology, Nara Medical University, School of Medicine, Kashihara, Nara 634-8521, Japan

ARTICLE INFO

Article history:
Received 8 February 2011
Available online 17 February 2011

Keywords:
A transmembrane receptor that has tyrosine kinase activity (c-kit)
Embryonic stem cell
Interstitial cells of Cajal (ICC)
Gut
Serotonin 4 receptor

ABSTRACT

Using an embryoid body (EB) culture system, we developed a functional organ-like cluster, a "gut", from mouse embryonic stem (ES) cells (ES gut). Each ES gut exhibited various types of spontaneous movements. In these spontaneously contracting ES guts, dense distributions of interstitial cells of Cajal (ICC) (c-kit, a transmembrane receptor that has tyrosine kinase activity, positive cells; gut pacemaker cells) and smooth muscle cells were discernibly identified, but enteric neural networks were not identified. In the present study, we succeeded in forming dense enteric neural networks by a 5-HT_4-receptor (SR4) agonist, mosapride citrate (1–10 μM) added only during EB formation. Addition of an SR4-antagonist, GR113808 (10 μM) abolished the SR4-agonist-induced formation of enteric neural networks. The SR4-agonist (1 μM) up-regulated the expression of mRNA of SR4 and the SR4-antagonist abolished this upregulation. 5-HT per se exerted similar effects to those of SR4-agonist, though less potent. These results suggest SR4-agonist differentiated enteric neural networks, mediated via activation of SR4 in the ES gut.

1. Introduction

Recently, embryonic stem (ES) cells were shown to spontaneously give rise to a functional organ-like unit, the "ES gut", which undergoes rhythmic contractions and is topographically comprised of enteric derivatives of all three embryonic germ layers: epithelial cells (endoderm), smooth muscle cells and interstitial cells of Cajal (ICCs; c-kit positive cells) (mesoderm), and a small number of diffusely distributed enteric neurons (ectoderm) [1]. On about day-21 of outgrowth culture, the ES gut begins to exhibit highly coordinated patterns of rhythmic motor activity comprised of periodic contractions and relaxations (phasic contraction); however, the motor patterns of those ES guts are not identical to gastrointestinal (GI) peristalsis [2]. Recent investigations have demonstrated that the ICC network within the musculature of the GI tract is responsible for the generation of electrical pacemaker activity and thus for the generation of rhythmic oscillations of the smooth muscle membrane potential called slow waves [3–8]. These oscillations in turn control the frequency and the propagation characteristics of GI motility [9–13].

Enteric neurons are also present within the GI tract; enteric neurons innervate the smooth muscle and are essential for peristalsis [14–16]. This suggests that enteric neurons might act in concert with ICCs to mediate the various patterns of GI motility [17–20]. Recently, we have been able to differentiate enteric neural network structures within the ES gut in the presence of exogenously added neurotrophic factors, brain-derived neurotrophic factor [21].

The aim of the present study was to reveal the role of a 5-HT_4-receptor (SR4) in differentiating enteric neurons and ICCs in ES guts. Mosapride citrate (Dainippon-Sumitomo Pharmaceuticals, Osaka, Japan) is a specific SR4 agonist, which enhanced enteric neural plasticity via enteric neural SR4 in *in vivo* distal gut [22]. We have thus investigated the effects of mosapride on differentiation of enteric neurons compared to ICCs in ES guts.

2. Materials and methods

2.1. ES cell culture

Undifferentiated ES cells (EB3) were maintained on gelatin-coated dishes without feeder cells in Dulbecco's modified Eagle's medium (DMEM; Sigma, St. Louis, MO) supplemented with 10% fetal bovine serum (FBS; GIBCO/BRL, Grand Island, NY), 0.1 mM 2-mercaptoethanol (Wako, Tokyo, Japan), 0.1 mM non-essential amino acids (GIBCO/BRL), 1 mM sodium pyruvate (Bio-WHITTAKER), and 1000 U/ml of LIF (CHEMICON, Temecula, CA). To induce

* Corresponding author. Fax: +81 744 23 4696.
E-mail address: mtakaki@naramed-u.ac.jp (M. Takaki).

0006-291X/$ - see front matter © 2011 Elsevier Inc. All rights reserved.
doi:10.1016/j.bbrc.2011.02.072

the embryoid body (EB) formation, dissociated ES cells were cultured in hanging drops as previously described with minor modifications [2]. Five-hundred cells were included per drop composed of 15 μl of ES cell-medium. In the medium, LIF was excluded and mosapride (1–10 μM) (kindly donated by Dainippon-Sumitomo Pharmaceutical Co. Ltd., Osaka, Japan) and/or GR113808 (10 μM) (GR; Wako Pure Chemical Industries, Osaka, Japan) were added. The formed EB was placed in outgrowth cultures on plastic dishes and allowed to attach [2]. On approximately day-13–18, the structures (ES guts) showed coordinated patterns of contraction with relatively regular rhythms.

2.2. Drugs

The following drugs were used: Mosapride citrate (kindly donated by Dainippon-Sumitomo Pharmaceutical Co. Ltd., Osaka, Japan), GR113808 (GR; Wako Pure Chemical Industries, Osaka, Japan), 5-Hydroxytryptamine hydrochloride (5-HT; Tokyo Chemical Industry, Tokyo, Japan). Mosapride and GR, dissolved in a solution containing 20% DMSO, were diluted to 100-fold with a final DMSO concentration of 0.2%. This concentration of DMSO did not exert any effects on experimental results.

2.3. Immunohistochemistry

For immunohistochemical detection of c-kit, a transmembrane receptor that has tyrosine kinase activity and neurofilament (NF), whole mount preparations of ES gut were fixed in acetone (4 °C, 5 min) [14]. After fixation, the preparations were washed for 30 min in PBS (0.01 M, pH 7.4) and then incubated for 3 h at room temperature in 10% normal goat serum in PBS containing 0.3% (v/v) Triton-X 100 (PBS-TX) to reduce nonspecific antibody binding. Tissues were then incubated either for two days at 4 °C with a rat monoclonal antibody raised against c-kit protein (ACK2, 5 μg/ml in PBS, eBioscience, San Diego, CA), with a rabbit polyclonal antiserum cocktail to label NF [2] and anti-serotonin receptor 4 (anti-SR4)(clone N-16, the epitope is located at the N-terminus of human SR-4, 0.5 μg/ml, Santa-Cruz Biotechnology Inc., Santa-Cruz, CA). Kit immunoreactivity was detected using an Alexa Flour®594-conjugated secondary antibody (Alexa Flour®594 goat anti-rat, Molecular Probes Inc., Eugene, OR; 1:200 in PBS for 2 h in the dark at room temperature). NF immunoreactivity was detected using a Texas Red-conjugated secondary antibody [2]. Tissues were examined with an OLYMPUS FV1000 (Tokyo, Japan) confocal microscope. Confocal micrographs are digital composites of Z-series scans of 10–15 optical sections through a depth of 10–20 μm or 100–150 μm. Final images were constructed with FV10-ASW [Ver1.6] (OLYMPUS).

2.4. Quantitative reverse transcription-polymerase chain reaction

The extraction of total RNA was carried out using RNeasy Mini Kit (Qiagen Genomics Inc., Bothell, WA) and total RNA (1 μg) was synthesized with the ReverTra Ace-α-RT Kit (Toyobo, Osaka, Japan). Quantitative reverse transcription-polymerase chain reaction (qRT-PCR) was performed by StepOne Real-Time PCR Systems (Applied Biosystems, Foster City, CA, USA) using Fast SYBR Green Master Mix (Applied Biosystems) and analyzed the relative standard curve quantification method. PCR condition was set according to the provider's instructions. Primers for mouse SR4 are 5′-ATG AGG ACA GAG ACC AA-3′ (upper) and 5′-AGC CAA GCC AGA GGA AA-3′ (lower) (GenBank accession No. NM008313). ACTB mRNA was amplified for internal control (GenBank accession No. NM001101). Each amplification reaction was evaluated by a melting curve analysis. For visualizing PCR products, agarose gel electrophoresis was performed with ethidium bromide staining.

3. Results and discussion

3.1. ES cell culture

We previously showed that ES cells can give rise to a functional organ-like unit, the ES gut, which consists of a broad array of enteric derivatives from all three embryonic germ layers, including various kinds of epithelial cells, smooth muscle cells and ICCs [1]. The morphological and physiological characteristics of ES guts that differentiate spontaneously from EBs in the absence of exogenous neurotrophic factors have been fully documented [2]; in those preparations, only few, if any, enteric neurons are observed [1,2].

We examined the formation process of EBs from ES cells during the hanging drop culture. After 6–7 day hanging drop culture, the formation into the EB dramatically occurred [21]. During hanging drop culture, c-kit was not found in 2 days, as previously reported [21]. However, in 4 days and the EB, several number of c-kit positive (+) cells were found after reexamination, although neural crest cell markers, c-ret, sox9 and p75 were not found [21,23]. Even after 2–3 weeks in outgrowth culture no neural crest cell markers, c-ret, sox9 and p75 were found in the ES gut without treatment with any trophic factors [21].

On the other hand, many number of c-kit positive (+) cells were detected after 2–3 weeks in outgrowth culture [21,23] without treatment with any trophic factors, suggesting that ICCs are spontaneously differentiated in the ES gut during at least 14–21 day outgrowth culture. It is predictable that formed ICCs mediate the spontaneous gut motility [17–20,24,25]. ES guts equipped with spontaneously differentiated ICCs demonstrated various types of spontaneous motility as previously reported [2], but did not peristalsis-like one.

3.2. Immunohistochemistry of ES gut

In the whole mount preparations of mouse embryonic stem cell (ES) guts differentiated from the embryoid body (EB) treated with a SR4-agonist, mosapride (1 μM), a group of neurofilament (NF) immunoreactive (+) cells and/or fibers formed neural networks within the wall of the dome-like structure (Fig. 1A) surrounding the lumen. In the ES gut from EB treated with DMSO alone, c-kit positive (+) cells were detected within the wall of the dome-like structure (Fig. 1B). In ES guts from EB treated with none or DMSO, no NF positive (+) cells and/or fibers were found (Fig. 2A), but in ES guts from EB treated with mosapride (1–10 μM), a group of NF positive (+) cells and/or fibers formed neural networks within the wall (Figs. 2B, C and 3A). Furthermore, spontaneously differentiated ICCs were also observed in these ES guts. One example was shown in Fig. 3A. ES guts equipped with both ICC and neural networks demonstrated peristalsis-like motility [21]. The peristalses observed in the mouse gut are conductive contractions from oral to anal side transporting intraluminal contents [18]. However, ES guts do not have their own orifice and so that no evacuation of intraluminal contents occurs. Therefore, peristalsis-like motility observed in the gut was somewhat different from the one observed in the mouse gut [18].

In ES guts from EB treated with an SR4-antagonist, GR113808 (GR; 10 μM) and mosapride (1–10 μM), no NF immunoreactive (+) cells and fibers were found but many number of c-kit positive (+) cells were detected (Fig. 3B). These ES guts demonstrated spontaneous motility, but did not peristalsis-like one. On the other hand, 5-HT per se facilitated differentiation of NF immunoreactive (+) cells and fibers (Fig. 3C), though less potently than a SR4 agonist. This ES gut equipped with neural and ICC networks also demonstrated peristalsis-like motility.

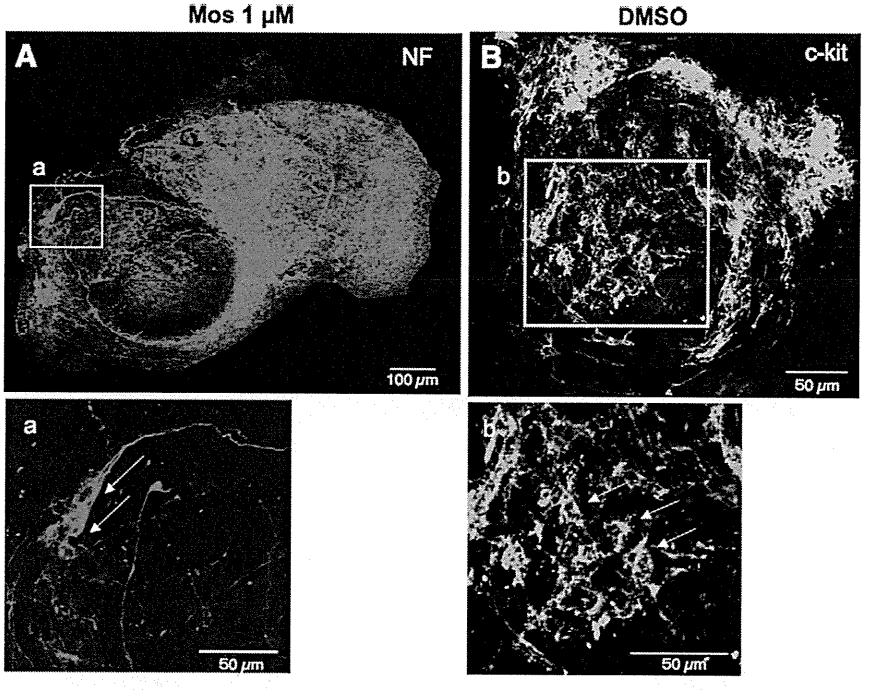

Fig. 1. Immunohistochemical detection of neurofilament (NF; A) and c-kit (B) in two dome-like structure ES guts after 14–21 day outgrowth culture differentiated from embryoid bodies (EBs) treated with 1 μM mosapride (A) and 0.2% dimethyl sulfoxide (DMSO) (B). a and b correspond to a area in A and b area in B, respectively. Arrows indicate neural cells (a) and ICCs (b), respectively.

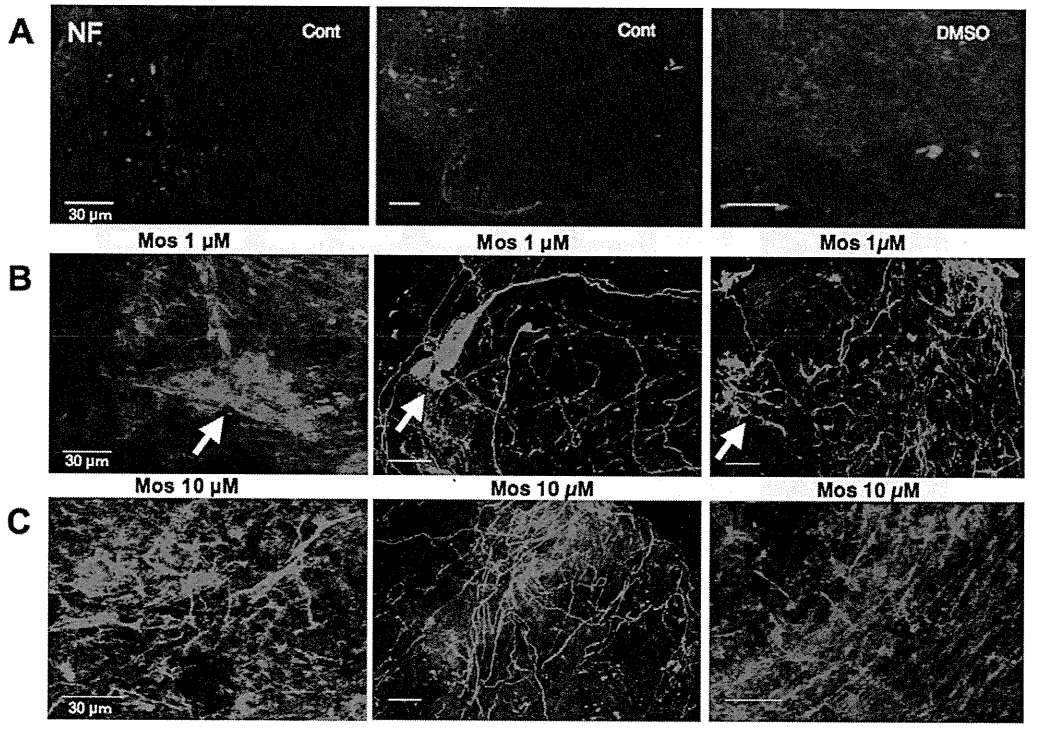

Fig. 2. Immunohistochemical detection of NF in each three different embryonic stem cell-derived guts (ES guts) after 14–21 day outgrowth culture from embryoid bodies (EBs) with no treatment (Cont) and 0.2% DMSO (A) and with 1 μM mosapride (B) and 10 μM mosapride (C). NF-positive cells and fibers (network) were found in B and C, but no NF+ cells were found in A. Each arrow in B indicates a ganglion.

The result presented here suggested the possibility that differentiation of NF immunoreactive (+) cells and fibers were facilitated by SR4. A part of NF-positive cells and fibers were also SR4-positive, supporting this possibility (Fig. 4A).

The mRNA expression of SR4 was significantly up-regulated by mosapride or 5-HT ($P < 0.001$), compared with that of control and by DMSO. 5-HT-induced up-regulation of the mRNA expression of SR4 was slightly less potent than SR4 agonist. SR4 antagonist,

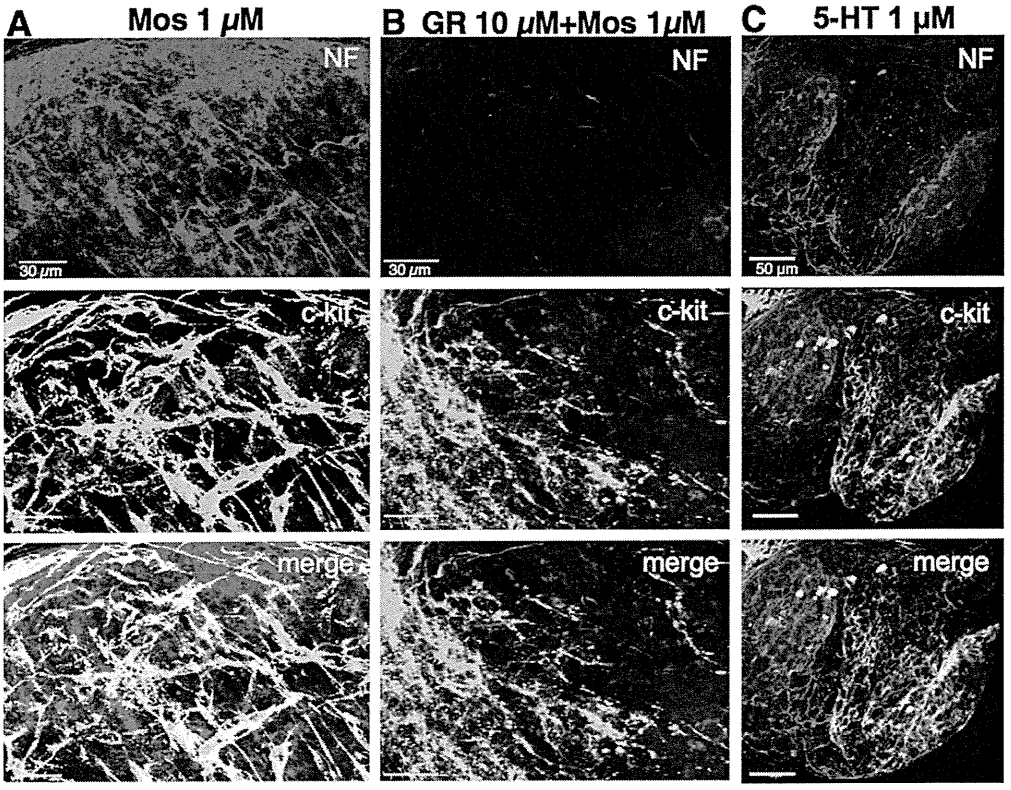

Fig. 3. Immunohistochemical detection of NF and c-kit in three ES guts after 14–21 day outgrowth culture differentiated from EBs treated with 1 μM mosapride (Mos)(A) and 10 μM GR113808 (GR), a 5-HT_4-receptor (SR4) blocker plus 1 μM Mos (B), and 1 μM 5-HT (C). NF-positive cells and fibers (network) and many c-kit+ cells forming network were found in A, C. Only c-kit+ cells forming network were found in B.

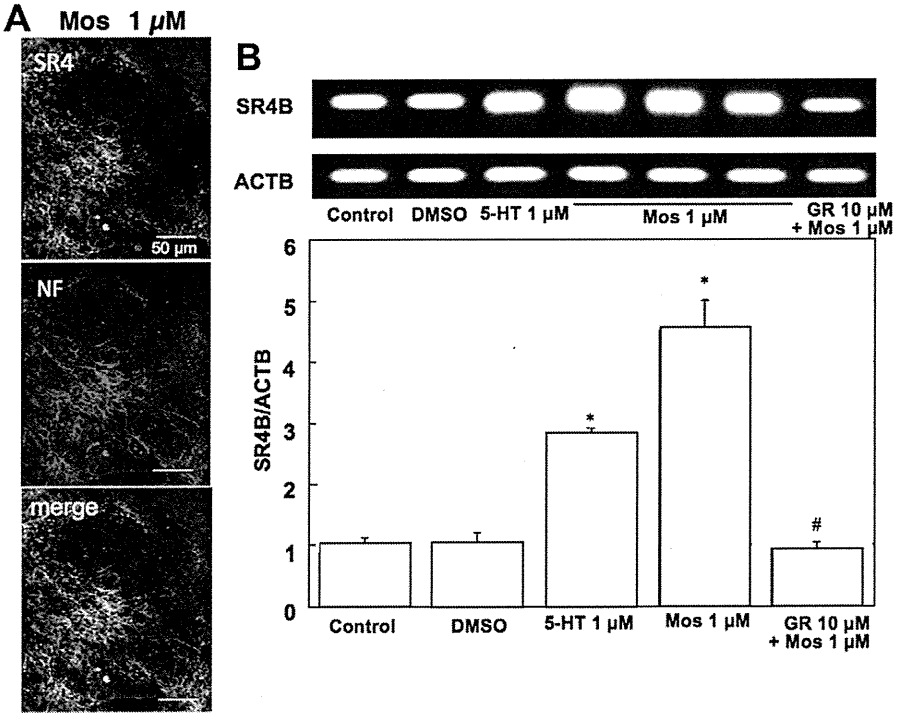

Fig. 4. (A) Immunohistochemical detection of NF and SR4 in an ES gut after 14-day outgrowth culture differentiated from EBs treated with 1 μM Mos. A part of NF-positive cells ware also SR4 positive. (B) Quantitative reverse transcription-polymerase chain reaction (qRT-PCR) for mRNA of SR4 in ES guts after 14–18 day outgrowth culture differentiated from EBs treated with no treatment (Control), DMSO, 5-HT 1 μM, Mos 1 μM and GR 10 μM + Mos 1 μM. Each qRT-PCR was repeated three times. Upper column indicates each band in ES guts in Control, DMSO, 5-HT 1 μM, Mos 1 μM ($n = 3$) and GR 10 μM + Mos 1 μM. ACTB: ß-actin. $^{*}P < 0.001$ vs. Control and DMSO; $^{\#}P < 0.001$ vs. Mos 1 μM

GR was significantly antagonized SR4-agonist induced up-regulation of mRNA expression of SR4 to the level of control and DMSO ($P < 0.001$) (Fig. 4B).

We have identified an ICC network in the ES gut, making it plausible that interactions between ICCs and smooth muscle cells lead to the spontaneous movements exhibited by the ES guts differentiated from EBs like in murine small intestine [17]. In the present in vitro study, spontaneous differentiation of ICC network and enteric neural network differentiated by a SR4 agonist in the ES gut made it plausible that interactions among ICCs, enteric neurons and smooth muscle cells lead to peristalsis-like contractions exhibited by the ES guts differentiated from EBs.

Moreover, in *in vivo* studies, it was shown that activation of enteric neural SR4 promotes reconstruction of an enteric neural circuit leading to the recovery of the defecation reflex in the distal gut [22]. It has also been shown that SR4 agonists play a role not only in the differentiation but also survival and neurogenesis of enteric neurons during development [26]. In the present study, it seems likely that application of SR4 increases differentiation of enteric neurons from ES cells possibly mediated via neural crest-derived precursors, but the possibility of SR4-mediated neuroprotection cannot be excluded. In addition, as the expression of 5-HT_{2B} receptors in the fetal enteric nervous system (ENS) of fetal mice and the role of 5-HT_{2B} receptors in the promotion of neuronal precursor differentiation of ENS during development have been described by Fiorica-Howells et al. [27], it seems likely that 5-HT_{2B} receptors also play a role in the enteric neuronal differentiation in ES gut-like structure.

Further studies would be needed to clarify underlying mechanisms for formation of enteric neural networks. Present results suggest a promising new *in vivo* pharmacotherapy for generating new enteric neurons to rescue aganglionic gut disorder.

4. Conclusions

We for the first time have succeeded in combining improved technology (EB culture) with appropriate addition of a 5-HT_4-receptor agonist to specifically facilitate differentiation of an ES gut equipped with enteric neural network structure with ICC. The ES gut without enteric neural network did not exhibit any peristalsis-like movements, even if ICC is differentiated. Accordingly, this ES gut model would be useful not only to investigate the roles of ICC and enteric neurons in the control of digestive motility but also to develop new drugs for pharmacotherapy for generating new enteric neurons to rescue aganglionic gut disorder.

Acknowledgments

This work was supported by Grants-in-aid for Scientific Research (14657311, 16650090 and 17300130 for MT) from the Ministry of Education, Science, Sports and Culture of Japan.

References

[1] T. Yamada, M. Yoshikawa, M. Takaki, S. Torihashi, Y. Kato, Y. Nakajima, S. Ishizaka, Y. Tsunoda, In vitro function gut-like organ formation from mouse embryonic stem cells, Stem Cells 20 (2002) 41–49.
[2] T. Ishikawa, S. Nakayama, T. Nakagawa, K. Horiguchi, H. Misawa, M. Kadowaki, A. Nakao, S. Inoue, T. Komuro, M. Takaki, Characterization of in vitro gutlike organ formed from mouse embryonic stem cells, Am. J. Physiol. Cell Physiol. 286 (2004) C1344–C1352.
[3] T. Der-Silaphet, J. Malysz, S. Hagel, A. Larry Arsenault, J.D. Huizinga, Interstitial cells of Cajal direct normal propulsive contractile activity in the mouse small intestine, Gastroenterology 114 (1998) 724–736.
[4] A. Fujita, T. Takeuchi, N. Saitoh, J. Hanai, F. Hata, Expression of Ca^{2+}-activated K^+ channels SK3 in the interstitial cells of Cajal in the gastrointestinal tract, Am. J. Physiol. Cell Physiol. 281 (2001) C1727–C1733.
[5] J.D. Huizinga, Y. Zhu, J. Ye, A. Molleman, High conductance chloride channels generate pacemaker currents in interstitial cells of Cajal, Gastroenterology 123 (2002) 1627–1636.
[6] J.C.F. Lee, L. Thuneberg, I. Berezin, J.D. Huizinga, Generation of slow waves in membrane potential is an intrinsic property of interstitial cells of Cajal, Am. J. Physiol. Gastrointest. Liver Physiol. 277 (1999) G409–G423.
[7] H. Suzuki, H. Takano, Y. Yamamoto, T. Komuro, M. Saito, K. Kato, K. Mikoshiba, Properties of gastric smooth muscles obtained from mice which lack inositol triphosphate receptor, J. Physiol. (Lond) 525 (2000) 105–111.
[8] L. Thomsen, T.L. Robinson, J.C. Lee, L.A. Farraway, D.W. Andrews, J.D. Huizinga, Interstitial cells of Cajal generate a rhythmic pacemaker current, Nat. Med. 4 (1998) 848–851.
[9] J.D. Huizinga, L. Thuneberg, M. Klüppel, J. Malysz, H.B. Mikkelsen, A. Bernstein, The W/kit gene required for interstitial cells of Cajal and for intestinal pacemaker activity, Nature 373 (1995) 347–349.
[10] K. Nakamura, Y. Shibata, Connexin43 expression in network-forming cells at the submucosal-muscular border of guinea pig and dog colon, Cell Tissues Organs 165 (1999) 16–21.
[11] K.M. Sanders, T. Ördög, S.D. Koh, S. Torihashi, S.M. Ward, Development and plasticity of interstitial cells of Cajal, Neurogastroenterol. Motil. 11 (1999) 311–338.
[12] S. Torihashi, S.M. Ward, K.M. Sanders, Development of c-Kit-positive cells and the onset of electrical rhythmicity in murine small intestine, Gastroenterology 112 (1997) 144–155.
[13] S. Yoneda, H. Takano, M. Takaki, H. Suzuki, Properties of spontaneously active cells distributed in the submucosal layer of mouse proximal colon, J. Physiol. (Lond) 542 (2002) 887–897.
[14] M. Costa, G.W. Hennig, S.J. Brookes, Intestinal peristalsis: a mammalian motor pattern controlled by enteric neural circuits, Ann. N. Y. Acad. Sci. 860 (1998) 464–466.
[15] T. Hukuhara, S. Kotani, G. Sato, Comparative studies on the motility of the normal denervated and aganlionic THIRY-loops, Jpn. J. Physiol. 12 (1962) 348–356.
[16] T. Hukuhara, T. Sumi, S. Kotani, The role of the ganglionic cells in the small intestine taken in the intestinal intrinsic reflex, Jpn. J. Physiol. 11 (1961) 281–288.
[17] T. Nakagawa, S. Ueshima, H. Fujii, Y. Nakajima, M. Takaki, Different modulation of spontaneous activities by nitrergic inhibitory nerves between ileum and jejunum in W/W^v mutant mice, Auton. Neurosci.: Basic and Clinical 119 (2005) 25–35.
[18] T. Nakagawa, H. Misawa, Y. Nakajima, M. Takaki, Absence of peristalsis in the ileum of W/W^v mutant mice that are selectively deficient in myenteric interstitial cells of Cajal, J. Smooth Muscle Res. 41 (2005) 141–151.
[19] S. Yoneda, H. Fukui, M. Takaki, Pacemaker activity from submucosal interstitial cells of Cajal drives high-frequent and low-amplitude circular muscle contractions in the mouse proximal colon, Neurogastroenterol. Motil. 16 (2004) 621–627.
[20] M. Takaki, S. Yoneda, T. Nakagawa, T. Ishikawa, Role of interstitial cells of Cajal and enteric neurons on gut spontaneous motility, Auton. Neurosci.: Basic and Clinical 106 (2003) 41.
[21] M. Takaki, S. Nakayama, H. Misawa, T. Nakagawa, H. Kuniyasu, In vitro formation of enteric neural network structure in a gut-like organ differentiated from mouse embryonic stem cells, Stem Cells 24 (2006) 1414–1422.
[22] H. Matsuyoshi, H. Kuniyasu, M. Okumura, H. Misawa, R. Katsui, G.-X. Zhang, K. Obata, M. Takaki, A 5-HT_4-receptor activation-induced neural plasticity enhances in vivo reconstructs of enteric nerve circuit insult, Neurogastroenterol. Motil. 22 (2010) 806. e226.
[23] M. Takaki, H. Misawa, J. Shimizu, H. Kuniyasu, K. Horiguchi, Inhibition of gut pacemaker cell formation from mouse ES cells by the c-kit inhibitor, Biochem. Biophys. Res. Commun. 359 (2007) 354–359.
[24] S.M. Ward, E.A. Beckett, X. Wang, F. Baker, M. Khoyi, K.M. Sanders, Interstitial cells of Cajal mediate cholinergic neurotransmission from enteric motor neurons, J. Neurosci. 20 (2000) 1393–1403.
[25] S.M. Ward, K.M. Sanders, G.D.S. Hirst, Role of interstitial cells of Cajal in neural control of gastrointestinal smooth muscles, Neurogastroenterol. Motil. 16 (Suppl.1) (2004) 112–117.
[26] M.-T. Liu, Y.-H. Kuan, J. Wang, R. Hen, M.D. Gershon, 5-HT_4 receptor-mediated neuroprotection and neurogenesis in the enteric nervous system of adult mice, J. Neurosci. 29 (2009) 9683–9699.
[27] E. Fiorica-Howells, L. Maroteaux, M.D. Gershon, Setotonin and the 5-HT_{2B} receptor in the development of enteric neurons, J. Neurosci. 20 (2000) 294–305.

Journal of General Virology (2011), 92, 2082–2087 DOI 10.1099/vir.0.032391-0

Short Communication

Structural requirements of virion-associated cholesterol for infectivity, buoyant density and apolipoprotein association of hepatitis C virus

Mami Yamamoto,[1,2] Hideki Aizaki,[1] Masayoshi Fukasawa,[3] Tohru Teraoka,[2] Tatsuo Miyamura,[1] Takaji Wakita[1] and Tetsuro Suzuki[1,4]

Correspondence
Tetsuro Suzuki
tesuzuki@hama-med.ac.jp

[1]Department of Virology II, National Institute of Infectious Diseases, Toyama 1-23-1, Shinjuku-ku, Tokyo 162-8640, Japan

[2]United Graduate School of Agricultural Science, Tokyo University of Agriculture and Technology, Saiwai-cho 3-5-8, Fuchu, Tokyo 183-8509, Japan

[3]Department of Biochemistry and Cell Biology, National Institute of Infectious Diseases, Toyama 1-23-1, Shinjuku-ku, Tokyo 162-8640, Japan

[4]Department of Infectious Diseases, Hamamatsu University School of Medicine, Handayama 1-20-1, Higashi-ku, Hamamatsu 431-3192, Japan

Received 22 March 2011
Accepted 17 May 2011

Our earlier study has demonstrated that hepatitis C virus (HCV)-associated cholesterol plays a key role in virus infectivity. In this study, the structural requirement of sterols for infectivity, buoyant density and apolipoprotein association of HCV was investigated further. We removed cholesterol from virions with methyl β-cyclodextrin, followed by replenishment with 10 exogenous cholesterol analogues. Among the sterols tested, dihydrocholesterol and coprostanol maintained the buoyant density of HCV and its infectivity, and 7-dehydrocholesterol restored the physical appearance of HCV, but suppressed its infectivity. Other sterol variants with a 3β-hydroxyl group or with an aliphatic side chain did not restore density or infectivity. We also provide evidence that virion-associated cholesterol contributes to the interaction between HCV particles and apolipoprotein E. The molecular basis for the effects of different sterols on HCV infectivity is discussed.

Hepatitis C virus (HCV) is a major cause of liver diseases, and is an enveloped, plus-strand RNA virus of the genus *Hepacivirus* of the family *Flaviviridae*. The mature HCV virion is considered to consist of a nucleocapsid, an outer envelope composed of the viral E1 and E2 proteins and a lipid membrane. Production and infection of several enveloped viruses, such as human immunodeficiency virus type 1 (HIV-1), hepatitis B virus and varicella-zoster virus (Bremer *et al.*, 2009; Campbell *et al.*, 2001; Graham *et al.*, 2003; Hambleton *et al.*, 2007), are dependent on cholesterol associated with virions. However, except for HIV-1 (Campbell *et al.*, 2002, 2004), there is limited information about the effects of replacing cholesterol with sterol analogues on the virus life cycle. We demonstrated the higher cholesterol content of HCV particles compared with host-cell membranes, and that HCV-associated cholesterol plays a key role in virion maturation and infectivity (Aizaki *et al.*, 2008). Recently, by using mass spectrometry, Merz *et al.* (2011) identified cholesteryl esters, cholesterol, phosphatidylcholine and sphingomyelin as major lipids of purified HCV particles.

To investigate further the effect of the structural requirement for cholesterol on the infectivity, buoyant density and apolipoprotein association of HCV, depletion of virion-associated cholesterol and substitution of endogenous cholesterol with structural analogues (Fig. 1a) was used in this study. HCVcc (HCV grown in cell culture) of the JFH-1 isolate (Wakita *et al.*, 2005), prepared as described previously (Aizaki *et al.*, 2008), was treated with 1 mM methyl β-cyclodextrin (B-CD), which extracts cholesterol from biological membranes, for 1 h at 37 °C. The cholesterol-depleted virus was then incubated with exogenous cholesterol or cholesterol analogues at various concentrations for 1 h. After removal of B-CD and free sterols by centrifugation at 38 000 r.p.m. (178 000 ***g***) for 2.5 h, the treated particles were used to infect Huh7 cells, kindly provided by Dr Francis V. Chisari (The Scripps Research Institute, La Jolla, CA, USA), and their infectivity was determined by quantifying the viral core protein in cells using an enzyme immunoassay (Ortho-Clinical Diagnostics) at 3 days post-infection (p.i.). Virus infectivity, which fell to <20 % after B-CD treatment, was

A supplementary table and figure are available with the online version of this paper.

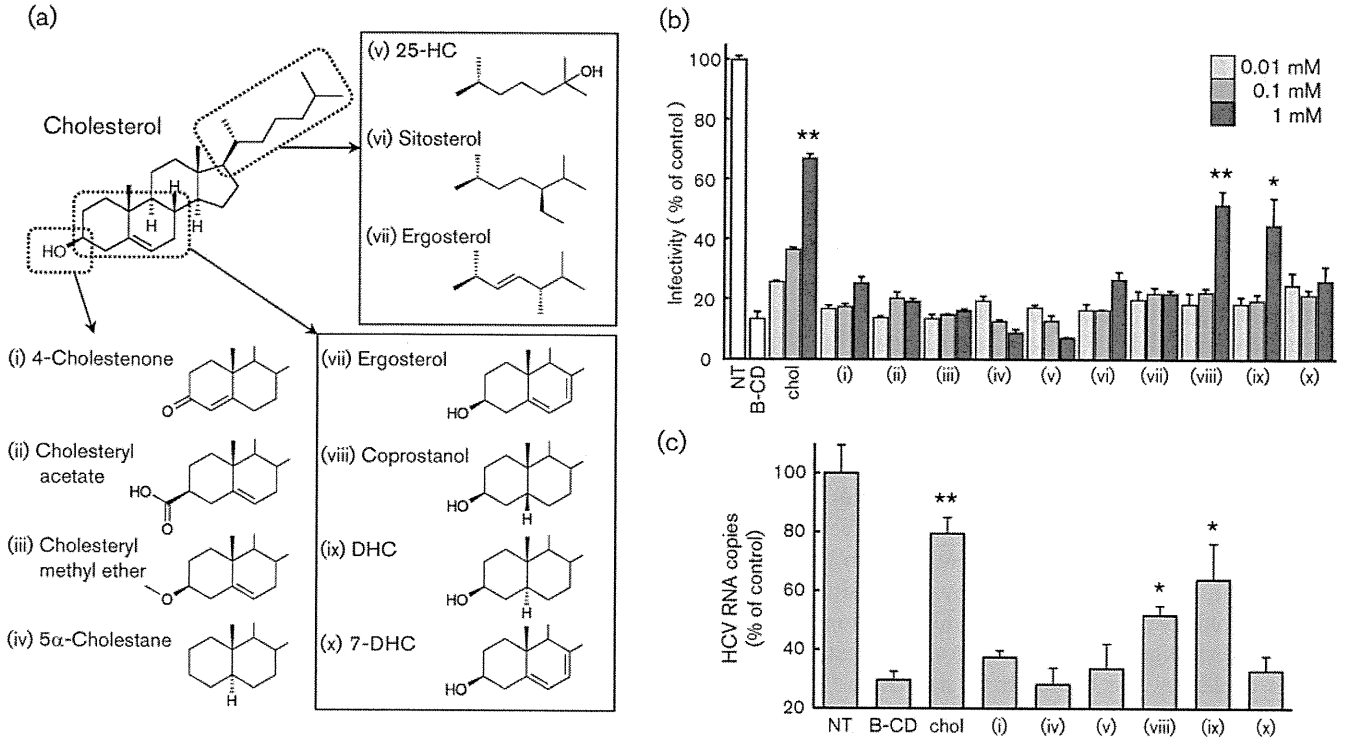

Fig. 1. Role of virion-associated cholesterol analogues in virus infection. (a) Structures of sterols used in this study. Variations in the 3β-hydroxyl group (lower left), aliphatic side chain (upper right) or ring structure (lower right) of cholesterol are shown. (i–x) Compounds studied in (b) and (c). (b) Effect of replenishment with sterols on HCV infectivity. Intracellular HCV core levels were determined at 72 h p.i. as the indicator of infectivity, which is represented as a percentage of the untreated HCVcc level (NT). (c) Effects of virion-associated sterols on virus internalization. HCV RNA copies in cells after virus internalization were quantified and are shown as percentages of the untreated HCVcc level (NT). (b, c) Means+SD of four samples are shown. *$P<0.05$; **$P<0.01$, compared with B-CD-treated virus (unpaired Student's t-test). Data are representative of at least two experiments.

recovered by addition of cholesterol at 0.01–1 mM in a dose-dependent manner (Fig. 1b). Among the cholesterol analogues tested, variants with a 3β-hydroxyl group (4-cholestenone, cholesteryl acetate, cholesteryl methyl ether and 5α-cholestane) or variants with an aliphatic side chain [25-hydroxycholesterol (25-HC), sitosterol and ergosterol] exhibited no or little effect on the recovery of infectivity of B-CD-treated HCV (Fig. 1b, lanes i–vii). In contrast, addition of variants in the structure of the sterol rings [coprostanol or dihydrocholesterol (DHC)] at 1 mM restored infectivity to around 50 % compared with non-treated virus control (Fig. 1b, lanes viii and ix). Other variants in the ring structure [7-dehydrocholesterol (7-DHC) and ergosterol, which is also a variant with an aliphatic side chain as indicated above] did not show any increase in the infectivity of B-CD-treated virus (Fig. 1b, lanes x and vii).

We demonstrated previously that HCV-associated cholesterol plays an important role in the internalization step of the virus, but not in cell attachment during virus entry (Aizaki *et al.*, 2008). The effect of virion-associated cholesterol analogues on virus attachment to cells and following internalization was determined. HCVcc, treated with B-CD with or without subsequent replenishment with sterols, was incubated with Huh7-25-CD81 cells, which stably express CD81 (Akazawa *et al.*, 2007), for 1 h at 4 °C. As an internalization assay, the incubation temperature was shifted to 37 °C post-binding procedure and maintained for 2 h. The cells were then treated with 0.25 % trypsin for 10 min at 37 °C, by which >90 % of HCV bound to the cell surface was removed (data not shown; Aizaki *et al.*, 2008). Internalized HCV was quantified by measuring the viral RNA in cell lysates by real-time RT-PCR (Takeuchi *et al.*, 1999). B-CD treatment or supplementation with sterols of B-CD-treated HCV had little or no effect on virus attachment to the cell surface (data not shown). Regarding virus internalization (Fig. 1c), treatment of HCVcc with 1 mM B-CD resulted in approximately 70 % reduction of viral RNA. The reduced level of the internalized HCV recovered markedly to approximately 80 % of the untreated HCVcc level by replenishment with 1 mM cholesterol. In agreement with the results shown in Fig. 1(b), addition of coprostanol or DHC to the B-CD-treated virus caused a significant recovery of virus internalization, suggesting that coprostanol and DHC associated with the

virion have the ability to play a role in HCV internalization into cells, in a manner comparable to cholesterol (Fig. 1c, lanes viii and ix). No or only a little recovery of virus internalization was observed by loading with other cholesterol analogues, such as 4-cholestenone, 5α-cholestane, 25-HC or 7-DHC (Fig. 1c, lanes i, iv, v and x).

To monitor the effect of cholesterol analogues on the physical characteristics of HCV, we next investigated buoyant-density profiles by using sucrose density-gradient centrifugation, in which untreated, B-CD-treated and sterol-replenished HCVcc were concentrated and layered onto continuous 10–60 % (w/v) sucrose density gradients, followed by centrifugation at 35 000 r.p.m. (151 000 *g*) for 14 h. Fractions were collected and analysed for the core protein. Fig. 2 shows that the virus density became higher after treatment with B-CD and that cholesterol-replenished virus shifted the density of B-CD-treated HCV to the non-treated level. Consistent with the result shown in Fig. 1(b), no effect on restoration of the buoyant densities of HCV was observed using variants with modifications in either the 3β-hydroxyl group (4-cholestenone, cholesteryl acetate and 5α-cholestane) or the aliphatic side chain (25-HC and sitosterol). In contrast, variants in the sterol ring structure (coprostanol, DHC and 7-DHC) had an ability to recover the density of B-CD-treated virus to that of non-treated virus.

Incorporation efficiency of the sterols into the cholesterol-depleted HCVcc was further determined by gas chromatography with flame ionization detection (see Supplementary Table S1, available in JGV Online). Under the experimental conditions used, exogenously supplied cholesterol after B-CD treatment was able to restore cholesterol content in HCVcc almost to initial levels. When 4-cholestenone, cholesteryl acetate, 25-HC, DHC or 7-DHC was added to B-CD-treated HCVcc, virion-associated sterol levels were 146, 157, 68, 96 or 73 %, respectively, of that of the non-treated control. The proportion of cholesterol analogues to the total sterols incorporated was ⩾30 % when 4-cholestenone, cholesteryl acetate, DHC or 7-DHC was used; however, the proportion in the case of 25-HC was only 3 %. It may be that the hydrophilic modification of the aliphatic side chain leads to poor association with HCVcc.

Collectively, exogenous variants with the 3β-hydroxyl group, such as 4-cholestenone and cholesteryl acetate, can be incorporated into B-CD-treated HCVcc, but resulted in no recovery of virus infectivity, indicating the importance of the 3β-hydroxyl group of cholesterol associated with the virus envelope in HCV infectivity. In contrast, two variants with modification in their sterol ring structures, coprostanol and DHC, have the ability to substitute for cholesterol. However, 7-DHC, another variant within the sterol ring, is incorporated readily into the depleted virion and restores the virus density, HCV replenished with 7-DHC is not infectious. These facts suggest that reduced forms of the sterol ring (coprostanol and DHC) in virion-associated cholesterol can be permitted for maintaining virus infectivity. However, a molecule with an additional double bond in the ring structure (7-DHC) seems to fail to exhibit infectivity, presumably because the change reduces structural flexibility in the

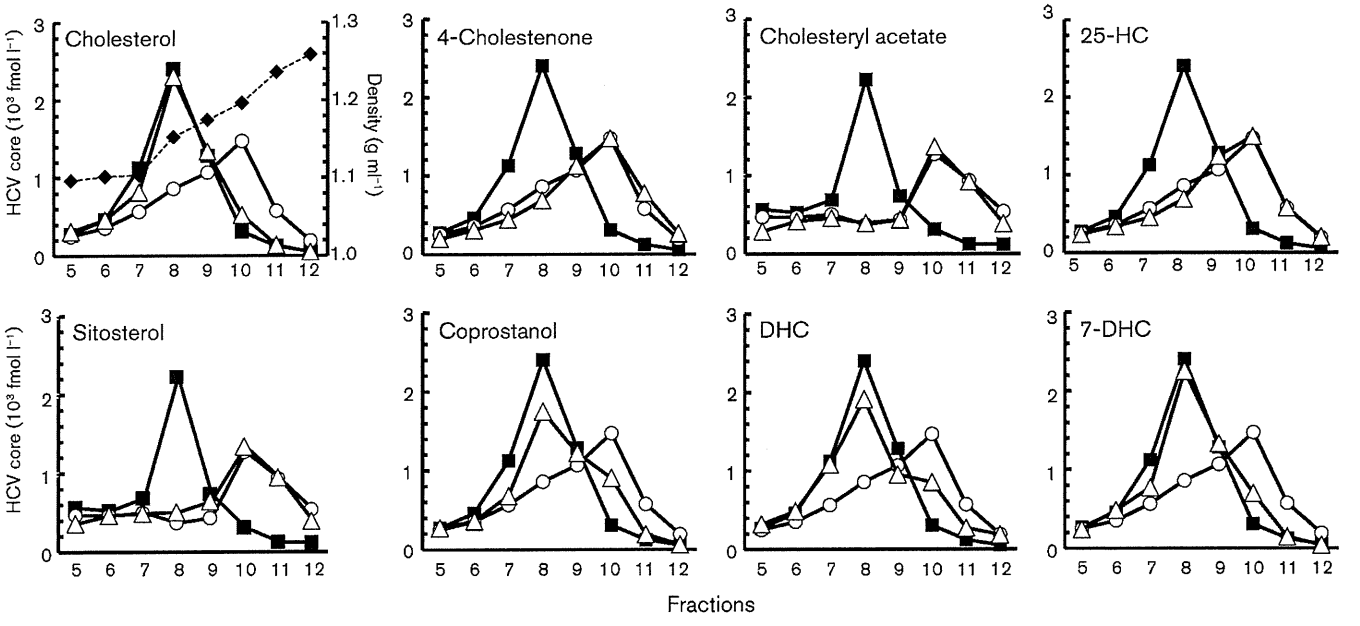

Fig. 2. Sucrose density-gradient profiles of lipid-modified HCV. Core protein concentration in each fraction of untreated HCVcc (■), B-CD-treated HCVcc (○) or HCVcc replenished with sterols (△) was determined. Corresponding densities of fractions are shown as a dashed line (◆).

sterol molecule and consequently in the virion structure. Coprostanol and DHC are *cis* and *trans* isomers, which are often known to have different physical properties. However, based on their molecular models, these two sterols, as well as cholesterol, possibly have similar spatial arrangements of the aliphatic side chain, the hydroxyl group and four-ring region because of their structural flexibility. In contrast, the spatial arrangement of 7-DHC does not seem comparable to that of cholesterol. Campbell *et al.* (2004) reported that replacement of HIV-1-associated cholesterol with raft-inhibiting sterols, including coprostanol, suppresses HIV-1 infectivity, whereas replacement with raft-promoting analogues such as DHC and 7-DHC (Megha *et al.*, 2006; Wang *et al.*, 2004; Xu & London, 2000; Xu *et al.*, 2001) maintains infectivity, demonstrating the importance of the raft-promoting properties of virion-associated cholesterol in HIV-1 infectivity (Campbell *et al.*, 2004). It is therefore likely that HCV-associated cholesterol is involved, at least in part, in virus infectivity via a molecular basis independent of lipid-raft formation.

The density of blood-circulating HCV is heterogeneous, ranging approximately from <1.06 to 1.25 g ml^{-1}, and it is proposed that low-density virus is associated with very-low-density lipoprotein (VLDL) and/or low-density lipoprotein (LDL) (André *et al.*, 2002; Thomssen *et al.*, 1993). It has recently been demonstrated that the pathway for VLDL assembly plays a role in assembly and maturation of infectious HCVcc (Icard *et al.*, 2009). HCVcc with low density, which is presumably associated with VLDL or VLDL-like lipoproteins, was found to possess higher infectivity than that with high density (Lindenbach *et al.*, 2006). This study, as well as our earlier work, indicated that removal of cholesterol from HCVcc by B-CD increased the buoyant density of the virus and reduced its infectivity. Thus, one may hypothesize that the virion-associated cholesterol plays a role in the formation of a complex with lipoproteins or apolipoproteins. To address this, the interaction between apolipoproteins and HCVcc with or without B-CD treatment was investigated by co-immunoprecipitation (Co-IP kit; Thermo Scientific). Virus samples were subjected separately to AminoLink Plus coupling resin, which was conjugated with a monoclonal antibody (mAb) against apolipoprotein E (ApoE) or apolipoprotein B (ApoB), and incubated at 4 °C for 4 h. After washing, total RNAs were extracted from the resulting resin beads by using TRIzol reagent (Invitrogen), followed by quantification of HCV RNA as described above (Takeuchi *et al.*, 1999). As indicated in Fig. 3(a), only a fraction of HCVcc was precipitated with an anti-ApoB mAb. In contrast, an anti-ApoE mAb was able to coprecipitate a considerable amount of the virus. It is of interest that B-CD-treated HCVcc hardly reacted with the mAb; however, the cholesterol-replenished virus was found to recover its reactivity, suggesting a role for virion-associated cholesterol in the formation of the HCV–lipoprotein/apolipoprotein complex. The results obtained are consistent with findings indicating that HCVcc can be captured with anti-ApoE antibodies, but capture with anti-ApoB antibodies is inefficient (Chang *et al.*, 2007; Hishiki *et al.*, 2010; Huang *et al.*, 2007; Jiang & Luo, 2009; Merz *et al.*, 2011; Nielsen *et al.*, 2006; Owen *et al.*, 2009), as well as with a recent model of structures of infectious HCV, in which HCVcc looks like ApoE-positive and primarily ApoB-negative lipoproteins (Bartenschlager *et al.*, 2011). We further tested the ApoE distribution in the density-gradient fractions of HCVcc samples (see Supplementary Fig. S1, available in JGV Online). With or without cholesterol depletion, ApoE was detected at a wide range of concentrations: 1.04 g ml^{-1} (fraction 1) to 1.17 g ml^{-1} (fraction 9). However, its level in the fractions at 1.10 g ml^{-1} (fraction 5) to approximately 1.17 g ml^{-1} was moderately decreased in the case of B-CD-treated virus.

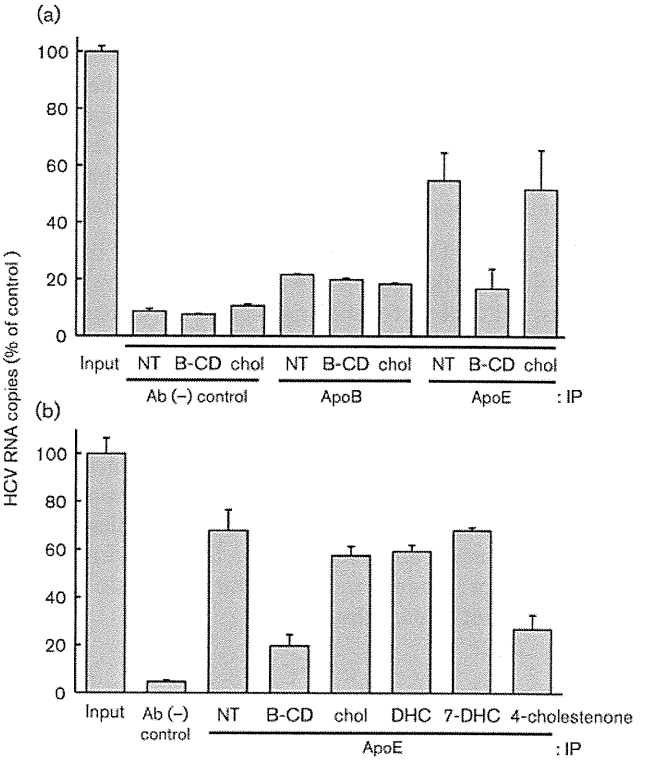

Fig. 3. Effect of virion-associated sterols on HCV–apolipoprotein interaction. (a) HCVcc samples with no treatment (NT), B-CD-treated (B-CD) or replenished with cholesterol (chol) were incubated with an amine-reactive resin coupling either an anti-ApoB mAb (ApoB) or an anti-ApoE mAb (ApoE). Control resin that is composed of the same material as above, but is not activated, was used as a negative control [Ab (–) control]. (b) B-CD-treated HCVcc was incubated with cholesterol (chol), DHC, 7-DHC or 4-cholestenone, followed by immunoprecipitation with the resin coupling with anti-ApoE mAb. (a, b) HCV RNAs in the immunoprecipitates were quantified and are indicated as percentages of the amount of input HCVcc RNA. Means+SD of three samples are shown. Data are representative of three experiments.

Whether cholesterol analogues could have a comparable role in HCV association with lipoprotein was examined further (Fig. 3b). Addition of DHC or 7-DHC, but not 4-cholestenone, to B-CD-treated HCVcc resulted in the recovery of coprecipitation of the virus with anti-ApoE. The results are correlated with the effect of sterols on the restoration of the buoyant densities of lipid-modified HCVcc (Fig. 2), suggesting that virion-associated cholesterol variants with modification in the sterol rings, but not in either the 3β-hydroxyl group or the aliphatic side chain, may tolerate the interaction between HCV and ApoE-positive lipoprotein.

Given that 7-DHC restored the association of HCV with ApoE and virion buoyant density, but did not restore infectivity, cholesterol and/or its analogues might affect the ability of virion membranes to fuse with the cell, independent of ApoE association. As cholesterol is an important mediator of membrane fluidity, one may hypothesize that HCV-associated cholesterol is involved in infectivity through modulation of the membrane fluidity. It has been reported that, in patients with Smith–Lemli–Opitz syndrome, a disorder of the cholesterol-synthesis pathway, cholesterol content decreases and 7-DHC increases in the cell membranes, leading to alteration of phospholipid packing in the membrane and abnormal membrane fluidity (Tulenko *et al.*, 2006).

It is now accepted that maturation and release of infectious HCV coincide with the pathway for producing VLDLs, which export cholesterol and triglyceride from hepatocytes. This study revealed roles for the structural basis of virion-associated cholesterol in the infectivity, buoyant density and apolipoprotein association of HCV. Although it was shown that HCV virions in infected patients, so-called lipo–viro particles, exhibited certain biochemical properties such as containing ApoB, ApoC and ApoE (Diaz *et al.*, 2006; Bartenschlager *et al.*, 2011), our studies provide useful information and the basis for future investigations toward a deeper understanding of the biogenesis pathway of infectious HCV particles.

Acknowledgements

We thank M. Matsuda, M. Sasaki and T. Date for technical assistance and T. Mizoguchi for secretarial work. This work was partially supported by a grant-in-aid for Scientific Research from the Japan Society for the Promotion of Science, from the Ministry of Health, Labor, and Welfare of Japan, and from the Ministry of Education, Culture, Sports, Science, and Technology.

References

Aizaki, H., Morikawa, K., Fukasawa, M., Hara, H., Inoue, Y., Tani, H., Saito, K., Nishijima, M., Hanada, K. & other authors (2008). Critical role of virion-associated cholesterol and sphingolipid in hepatitis C virus infection. *J Virol* **82**, 5715–5724.

Akazawa, D., Date, T., Morikawa, K., Murayama, A., Miyamoto, M., Kaga, M., Barth, H., Baumert, T. F., Dubuisson, J. & Wakita, T. (2007). CD81 expression is important for the permissiveness of Huh7 cell clones for heterogeneous hepatitis C virus infection. *J Virol* **81**, 5036–5045.

André, P., Komurian-Pradel, F., Deforges, S., Perret, M., Berland, J. L., Sodoyer, M., Pol, S., Bréchot, C., Paranhos-Baccalà, G. & Lotteau, V. (2002). Characterization of low- and very-low-density hepatitis C virus RNA-containing particles. *J Virol* **76**, 6919–6928.

Bartenschlager, R., Penin, F., Lohmann, V. & André, P. (2011). Assembly of infectious hepatitis C virus particles. *Trends Microbiol* **19**, 95–103.

Bremer, C. M., Bung, C., Kott, N., Hardt, M. & Glebe, D. (2009). Hepatitis B virus infection is dependent on cholesterol in the viral envelope. *Cell Microbiol* **11**, 249–260.

Campbell, S. M., Crowe, S. M. & Mak, J. (2001). Lipid rafts and HIV-1: from viral entry to assembly of progeny virions. *J Clin Virol* **22**, 217–227.

Campbell, S. M., Crowe, S. M. & Mak, J. (2002). Virion-associated cholesterol is critical for the maintenance of HIV-1 structure and infectivity. *AIDS* **16**, 2253–2261.

Campbell, S., Gaus, K., Bittman, R., Jessup, W., Crowe, S. & Mak, J. (2004). The raft-promoting property of virion-associated cholesterol, but not the presence of virion-associated Brij 98 rafts, is a determinant of human immunodeficiency virus type 1 infectivity. *J Virol* **78**, 10556–10565.

Chang, K. S., Jiang, J., Cai, Z. & Luo, G. (2007). Human apolipoprotein E is required for infectivity and production of hepatitis C virus in cell culture. *J Virol* **81**, 13783–13793.

Diaz, O., Delers, F., Maynard, M., Demignot, S., Zoulim, F., Chambaz, J., Trépo, C., Lotteau, V. & André, P. (2006). Preferential association of hepatitis C virus with apolipoprotein B48-containing lipoproteins. *J Gen Virol* **87**, 2983–2991.

Graham, D. R., Chertova, E., Hilburn, J. M., Arthur, L. O. & Hildreth, J. E. (2003). Cholesterol depletion of human immunodeficiency virus type 1 and simian immunodeficiency virus with β-cyclodextrin inactivates and permeabilizes the virions: evidence for virion-associated lipid rafts. *J Virol* **77**, 8237–8248.

Hambleton, S., Steinberg, S. P., Gershon, M. D. & Gershon, A. A. (2007). Cholesterol dependence of varicella-zoster virion entry into target cells. *J Virol* **81**, 7548–7558.

Hishiki, T., Shimizu, Y., Tobita, R., Sugiyama, K., Ogawa, K., Funami, K., Ohsaki, Y., Fujimoto, T., Takaku, H. & other authors (2010). Infectivity of hepatitis C virus is influenced by association with apolipoprotein E isoforms. *J Virol* **84**, 12048–12057.

Huang, H., Sun, F., Owen, D. M., Li, W., Chen, Y., Gale, M., Jr & Ye, J. (2007). Hepatitis C virus production by human hepatocytes dependent on assembly and secretion of very low-density lipoproteins. *Proc Natl Acad Sci U S A* **104**, 5848–5853.

Icard, V., Diaz, O., Scholtes, C., Perrin-Cocon, L., Ramière, C., Bartenschlager, R., Penin, F., Lotteau, V. & André, P. (2009). Secretion of hepatitis C virus envelope glycoproteins depends on assembly of apolipoprotein B positive lipoproteins. *PLoS One* **4**, e4233.

Jiang, J. & Luo, G. (2009). Apolipoprotein E but not B is required for the formation of infectious hepatitis C virus particles. *J Virol* **83**, 12680–12691.

Lindenbach, B. D., Meuleman, P., Ploss, A., Vanwolleghem, T., Syder, A. J., McKeating, J. A., Lanford, R. E., Feinstone, S. M., Major, M. E. & other authors (2006). Cell culture-grown hepatitis C virus is infectious *in vivo* and can be recultured *in vitro*. *Proc Natl Acad Sci U S A* **103**, 3805–3809.

Megha, Bakht, O. & London, E. (2006). Cholesterol precursors stabilize ordinary and ceramide-rich ordered lipid domains (lipid

rafts) to different degrees. Implications for the Bloch hypothesis and sterol biosynthesis disorders. *J Biol Chem* **281**, 21903–21913.

Merz, A., Long, G., Hiet, M. S., Brügger, B., Chlanda, P., Andre, P., Wieland, F., Krijnse-Locker, J. & Bartenschlager, R. (2011). Biochemical and morphological properties of hepatitis C virus particles and determination of their lipidome. *J Biol Chem* **286**, 3018–3032.

Nielsen, S. U., Bassendine, M. F., Burt, A. D., Martin, C., Pumeechockchai, W. & Toms, G. L. (2006). Association between hepatitis C virus and very-low-density lipoprotein (VLDL)/LDL analyzed in iodixanol density gradients. *J Virol* **80**, 2418–2428.

Owen, D. M., Huang, H., Ye, J. & Gale, M., Jr (2009). Apolipoprotein E on hepatitis C virion facilitates infection through interaction with low-density lipoprotein receptor. *Virology* **394**, 99–108.

Takeuchi, T., Katsume, A., Tanaka, T., Abe, A., Inoue, K., Tsukiyama-Kohara, K., Kawaguchi, R., Tanaka, S. & Kohara, M. (1999). Real-time detection system for quantification of hepatitis C virus genome. *Gastroenterology* **116**, 636–642.

Thomssen, R., Bonk, S. & Thiele, A. (1993). Density heterogeneities of hepatitis C virus in human sera due to the binding of beta-lipoproteins and immunoglobulins. *Med Microbiol Immunol (Berl)* **182**, 329–334.

Tulenko, T. N., Boeze-Battaglia, K., Mason, R. P., Tint, G. S., Steiner, R. D., Connor, W. E. & Labelle, E. F. (2006). A membrane defect in the pathogenesis of the Smith–Lemli–Opitz syndrome. *J Lipid Res* **47**, 134–143.

Wakita, T., Pietschmann, T., Kato, T., Date, T., Miyamoto, M., Zhao, Z., Murthy, K., Habermann, A., Kräusslich, H. G. & other authors (2005). Production of infectious hepatitis C virus in tissue culture from a cloned viral genome. *Nat Med* **11**, 791–796.

Wang, J., Megha & London, E. (2004). Relationship between sterol/steroid structure and participation in ordered lipid domains (lipid rafts): implications for lipid raft structure and function. *Biochemistry* **43**, 1010–1018.

Xu, X. & London, E. (2000). The effect of sterol structure on membrane lipid domains reveals how cholesterol can induce lipid domain formation. *Biochemistry* **39**, 843–849.

Xu, X., Bittman, R., Duportail, G., Heissler, D., Vilcheze, C. & London, E. (2001). Effect of the structure of natural sterols and sphingolipids on the formation of ordered sphingolipid/sterol domains (rafts). Comparison of cholesterol to plant, fungal, and disease-associated sterols and comparison of sphingomyelin, cerebrosides, and ceramide. *J Biol Chem* **276**, 33540–33546.

Hepatitis C Virus Reveals a Novel Early Control in Acute Immune Response

Noëlla Arnaud[1], Stéphanie Dabo[1], Daisuke Akazawa[2], Masayoshi Fukasawa[3], Fumiko Shinkai-Ouchi[3], Jacques Hugon[4], Takaji Wakita[2], Eliane F. Meurs[1]*

1 Institut Pasteur, Hepacivirus and Innate Immunity, Paris, France, **2** National Institute of Infectious Diseases, Department of Virology II, Tokyo, Japan, **3** National Institute of Infectious Diseases, Department of Biochemistry and Cell Biology, Tokyo, Japan, **4** Institut du Fer à Moulin, INSERM UMRS 839, Paris, France

Abstract

Recognition of viral RNA structures by the intracytosolic RNA helicase RIG-I triggers induction of innate immunity. Efficient induction requires RIG-I ubiquitination by the E3 ligase TRIM25, its interaction with the mitochondria-bound MAVS protein, recruitment of TRAF3, IRF3- and NF-κB-kinases and transcription of Interferon (IFN). In addition, IRF3 alone induces some of the Interferon-Stimulated Genes (ISGs), referred to as early ISGs. Infection of hepatocytes with Hepatitis C virus (HCV) results in poor production of IFN despite recognition of the viral RNA by RIG-I but can lead to induction of early ISGs. HCV was shown to inhibit IFN production by cleaving MAVS through its NS3/4A protease and by controlling cellular translation through activation of PKR, an eIF2α-kinase containing dsRNA-binding domains (DRBD). Here, we have identified a third mode of control of IFN induction by HCV. Using HCVcc and the Huh7.25.CD81 cells, we found that HCV controls RIG-I ubiquitination through the di-ubiquitine-like protein ISG15, one of the early ISGs. A transcriptome analysis performed on Huh7.25.CD81 cells silenced or not for PKR and infected with JFH1 revealed that HCV infection leads to induction of 49 PKR-dependent genes, including ISG15 and several early ISGs. Silencing experiments revealed that this novel PKR-dependent pathway involves MAVS, TRAF3 and IRF3 but not RIG-I, and that it does not induce IFN. Use of PKR inhibitors showed that this pathway requires the DRBD but not the kinase activity of PKR. We then demonstrated that PKR interacts with HCV RNA and MAVS prior to RIG-I. In conclusion, HCV recruits PKR early in infection as a sensor to trigger induction of several IRF3-dependent genes. Among those, ISG15 acts to negatively control the RIG-I/MAVS pathway, at the level of RIG-I ubiquitination.These data give novel insights in the machinery involved in the early events of innate immune response.

Citation: Arnaud N, Dabo S, Akazawa D, Fukasawa M, Shinkai-Ouchi F, et al. (2011) Hepatitis C Virus Reveals a Novel Early Control in Acute Immune Response. PLoS Pathog 7(10): e1002289. doi:10.1371/journal.ppat.1002289

Editor: Aleem Siddiqui, University of California, San Diego, United States of America

Received April 5, 2011; **Accepted** August 13, 2011; **Published** October 13, 2011

Funding: NA was supported by a graduate fellowship from the Ministry of Research and Technology. The work was supported by grants from the Pasteur Institute and by grant R750159 from ANRS (Agence Nationale de la Recherche sur le SIDA et les Hepatites Virales):http://www.anrs.fr The funders had no role in study design, data collection and analysis, decision to publish, or preparation of the manuscript.

Competing Interests: The authors have declared that no competing interests exist.

* E-mail: emeurs@pasteur.fr

Introduction

IFN induction in response to several RNA viruses involves the intracytosolic pathogen recognition receptor (PRR) CARD-containing DexD/H RNA helicase RIG-I. Following its binding to viral RNA, RIG-I undergoes a change in its conformation through Lys63-type ubiquitination by the E3 ligase TRIM25. This allows its N-terminal CARD domain to interact with the CARD domain of the mitochondria-bound adapter MAVS [1,2]. MAVS then interacts with TRAF3 to further recruit downstream IRF3 and NF-κB-activating kinases, that stimulate the IFNβ promoter in a cooperative manner. In addition, IRF3 stimulates directly the promoters of some interferon-induced genes (early ISGs) while NF-κB stimulates that of inflammatory cytokines [3].

The RNA of Hepatitis C virus (HCV) has an intrinsic ability to trigger IFNβ induction through RIG-I [4,5,6]. Yet HCV is a poor IFN inducer. One reason for this comes from the ability of its NS3 protease to cleave MAVS [7]. Another relates to the ability of HCV to trigger activation of the dsRNA-dependent eIF2α kinase PKR [8,9] which leads to inhibition of IFN expression through general control of translation while the viral genome can be translated from its eIF2α-insensitive IRES structure [8].

HCV infection can trigger important intrahepatic synthesis of several IFN-induced genes (ISGs) in patients [10,11] and in animal models of infection in chimpanzees [12]. Expression of ISGs can be explained at least in part by the ability of HCV to activate the IFN-producing pDCs in the liver through cell-to-cell contact with HCV-infected cells [13]. Intriguingly, despite the recognized antiviral activity of a number of these ISGs, their high expression paradoxically represents a negative predictive marker for the response of these patients to standard combination IFN/ribavirin therapy [14,15,16]. The ubiquitine-like protein ISG15 is among the ISGs which are the most highly induced by HCV [16] and was recently shown to act as a pro-HCV agent [17]. Interestingly, ISG15 was also shown to control RIG-I activity through ISGylation [18].

Here, we show that HCV controls IFN induction at the level of RIG-I ubiquitination through the ubiquitine-like protein ISG15, one of the early ISGs. Use of small interfering RNA (siRNA) targeting to compare the effect of ISG15 to that of PKR on IFN induction and HCV replication led to the unexpected finding that HCV infection triggers induction of ISG15 and other ISGs by using PKR as an adapter through its N terminal dsRNA binding domain. This recruits a signaling pathway which involves MAVS,TRAF3

Author Summary

Hepatitis C Virus (HCV) is a poor interferon (IFN) inducer, despite recognition of its RNA by the cytosolic RNA helicase RIG-I. This is due in part through cleavage of MAVS, a downstream adapter of RIG-I, by the HCV NS3/4A protease and through activation of the eIF2α-kinase PKR to control IFN translation. Here, we show that HCV also inhibits RIG-I activation through the ubiquitin-like protein ISG15 and that HCV triggers rapid induction of 49 genes, including ISG15, through a novel signaling pathway that precedes RIG-I and involves PKR as an adapter to recruit MAVS. Hence, we propose to divide the acute response to HCV infection into one early (PKR) and one late (RIG-I) phase, with the former controlling the latter. Furthermore, these data emphazise the need to check compounds designed as immune adjuvants for activation of the early acute phase before using them to sustain innate immunity.

and IRF3 but not RIG-I. Altogether, our results present a novel mechanism by which HCV uses PKR and ISG15 to attenuate the innate immune response.

Results

HCV infection negatively controls RIG-I ubiquitination

We recently reported that the HCV permissive Huh7.25.CD81 cells [19] that we used to identify the pro-HCV action of PKR, did not induce IFN in response to HCV infection, unless after ectopic expression of TRIM25 [8]. We started this study by investigating at which level this defect could occur. A $P_{358}L$ substitution in the endogenous TRIM25 of these cells, revealed by sequence analysis, proved to have no incidence of the ability of TRIM25 to participate in the IFN induction process. Indeed, ectopic expression of a TRIM25 $P_{358}L$ construct was as efficient as a TRIM25wt construct to increase IFN induction in the Huh7.25.CD81 cells, after infection with Sendai virus (SeV) (**Figure 1A**). Like some other members of the TRIM family, TRIM25 is localized in both the cytosol and nucleus and is induced upon IFN treatment [20]. No specific difference between the cellular localization of TRIM25 was observed in the Huh7.25.CD81 cells when compared to Huh7 cells or Huh7.5 cells, which rules out a role for a cellular mislocalization in its inability to participate in IFN induction (**Figure 1B**). TRIM25 was also efficiently induced by IFN (**Figure 1B and Figure S1**). We assayed whether increasing TRIM25 upon IFN treatment could mimic the effect of its ectopic expression and restore IFN induction in response to HCV infection. However, this resulted only in a poor stimulation of an IFNβ promoter (3 to 5-fold), in contrast to its effect upon SeV infection (230-fold) (**Figure 1C**). Similarly, HCV infection at higher m.o.i, as an attempt to favour recognition of RIG-I by the viral RNA, only modestly increased IFN induction (**Figure 1D**). TRIM25 plays an essential role in IFN induction through RIG-I ubiquitination [1]. We then analysed whether this step was affected by HCV infection in the Huh7.25.CD81 cells. The results showed that, in contrast to SeV infection used as control, HCV infection could not trigger RIG-I ubiquitination, unless the cells are supplied with ectopic TRIM25 (**Figure 1E**). Thus, HCV infection appears to mediate a control on IFN induction through regulation of RIG-I ubiquitination.

HCV controls RIG-I ubiquitination through ISG15

Inhibition of the function of TRIM25 or RIG-I ubiquitination has been suggested to occur via the small ubiquitin-like protein ISG15 and the process of ISGylation [18,21]. We then analysed whether ISG15 was involved in the control of RIG-I ubiquitination upon HCV infection. For this, we chose a transient transfection approach using siRNAs targeting ISG15 in the Huh7.25.CD81 cells. Indeed, this resulted in a strong ubiquitination of RIG-I at 9 hrs and 12 hrs post-HCV infection, which was equivalent to that observed in cells supplied with ectopic TRIM25 (**Figure 2A**). A similar result was obtained after JFH1 infection in the Huh7 cells, used as another HCV-permissive cell line (**Figure S2**). Thus, ISG15 can control RIG-I ubiquitination in different cells infected by HCV. We next investigated whether ISGylation was involved in this process. Absence of detection of RIG-I ubiquitination after HCV infection of the Huh7.25.CD81 cells precludes direct analysis of the effect of ISG15 on RIG-I. We used an IFNβ-luc reporter assay instead, as it proved to be sensitive enough to detect some IFN induction in response to JFH1 infection in those cells (see Figure 1D). We found that IFN induction increased when cells were transfected with siRNAs targeting ISG15 while it decreased in cells overexpressing IGS15 (**Figure 2B**). Expression of ISG15 in the presence of the E1, E2 and E3 ligases involved in ISGylation (respectively Ube1L, UbcH8 and HERC5) [22] further inhibits IFNβ induction (**Figure 2B**). Similar results were observed upon infection with Sendai virus (**Figure S3**). The ISGylation process is strictly dependent on the presence of the E1 ligase Ube1L [23]. Indeed, enhanced IFN promoter activity has been observed in Ube1L−/− cells in response to NDV [18]. In accord with this, depletion of endogenous Ube1L from the Huh7.25.CD81 cells (**Figure S4**), as such or after ectopic expression of ISG15, UbcH8 and HERC5, resulted in an increase in IFNβ induction after infection with HCV (**Figure 2B**). We then analysed the effect of siISG15 on IFNβ induction after infecting the cells with HCV up to 72 hours, in order to pass through the 24 hr time-point where the signaling pathway leading to the transcription of this gene is expected to stop because of the NS3/4A-mediated cleavage of MAVS [8]. The results show that, whereas IFNβ transcription was indeed strongly inhibited after 24 hr in the control cells, it still occurred significantly in the cells expressing siRNA ISG15 (**Figure 2C**). Previous data have shown a positive role for ISG15 on HCV production [24,25]. In accord with this, silencing of ISG15 resulted in clear inhibition of HCV RNA expression with however no significant consequence on the ability of the virions produced to re-infect fresh cells (**Figure 2D**). Analysis of expression of MAVS and NS3, as well as the expression of the core protein as another example of viral protein, then showed that the depletion of ISG15 both decreased and delayed the expression of the viral proteins as compared to the siRNA control cells and that this was correlated by a delay in the NS3/4A-mediated cleavage of MAVS (**Figure 2E**). These results show that ISG15 controls the process of IFN induction during HCV infection by interfering with RIG-I ubiquitination through an ISGylation process and by boosting efficient accumulation of NS3, among other viral proteins, thus favouring its negative control on IFN induction by cleavage of MAVS.

ISG15 strengthens the pro-HCV activity of PKR

ISG15 ([24,25] and this study) and PKR [8,9] emerge as two ISGs with pro-HCV activities, instead of playing an antiviral role. We then assayed the effect of a combined depletion of PKR and ISG15 on HCV replication and IFN expression in the Huh7.25.CD81 cells. As shown in Figure 2 D and B, siRNAs targeting ISG15 were sufficient both to inhibit HCV replication (**Figure 3A**) and to increase IFNβ expression, either measured by RTqPCR (**Figure 3B**) or by using an IFNβ-luciferase reporter

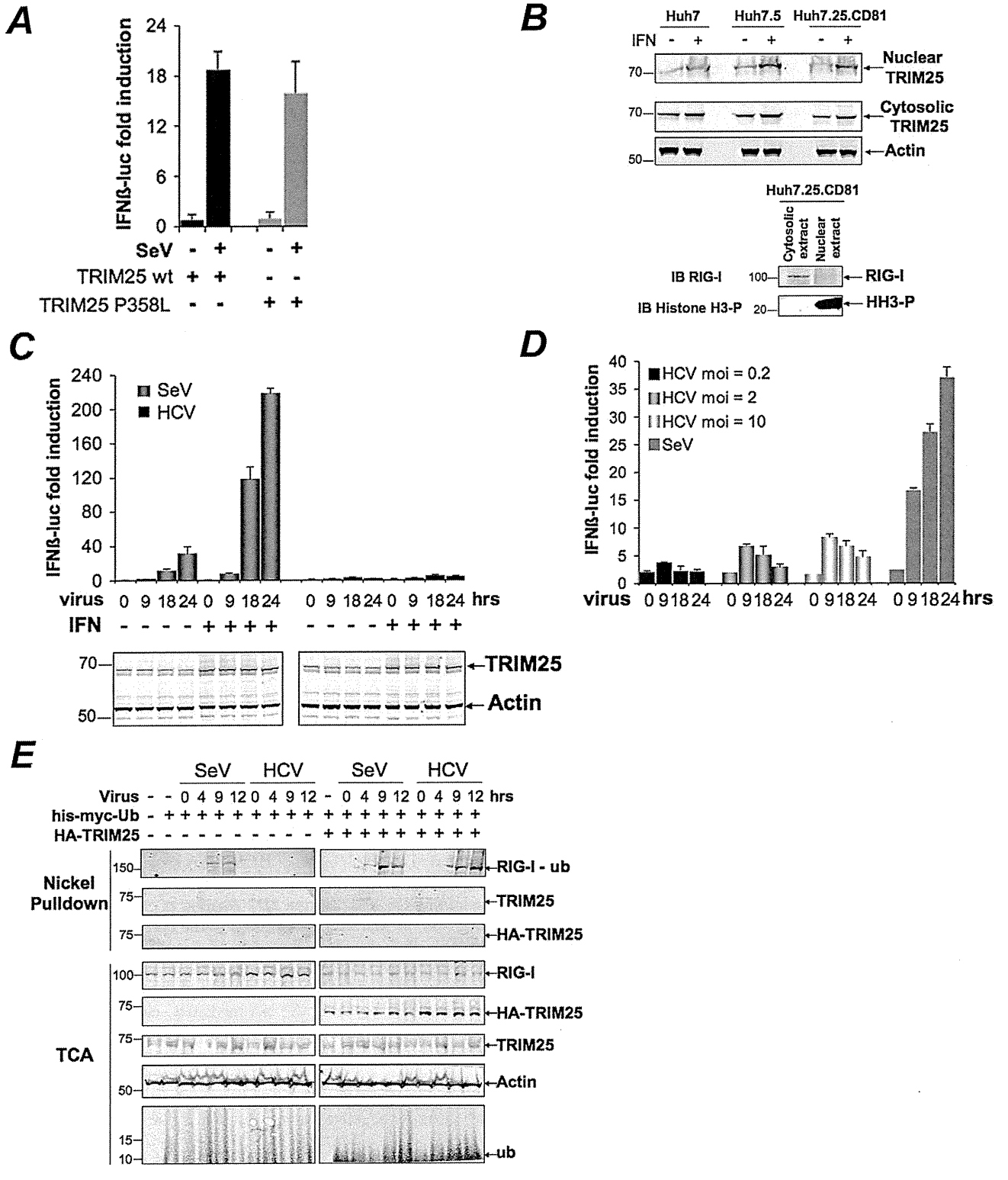

Figure 1. HCV infection negatively controls RIG-I ubiquitination. (**A**) Huh7.25.CD81 cells were transfected for 24 hrs with 150 ng of the pGL2-IFNβ-FLUC; 40 ng of the pRL-TK-RLUC reporter plasmids alone or in presence of 150 ng of a plasmid expressing HA-TRIM25, either as such (TRIM25wt) or containing the $P_{358}L$ substitution (a SNP rs75467764 with no reported pathology). Cells were infected or not with SeV (40 HAU/ml) for 24 hrs. IFN expression was expressed as fold induction of luciferase activity. Error bars represent the mean ± S.D. for triplicates. (**B**) Huh7, Huh7.5 and Huh7.25.CD81 cells were either untreated or treated with 500 U/ml IFNα for 24 hrs. TRIM25 was detected by immunoblot after preparation of nuclear and cytosolic fractions from 25 µg of cell extracts. Detection of Actin, RIG-I and phosphorylated Histone 3 (HH3-P) served as controls. (**C–D**) Huh7.25.CD81 cells were transfected with the reporter plasmids as in A, a few hours before being treated with 500 U/ml IFNα for 24 hrs (**C**) or left untreated (**C or D**). They were then infected with Sendai virus (40 HAU/ml) or with JFH1 at an m.o.i of 0.2 (**C**) or increasing from 0.2 to 10 (**D**). At the times indicated, IFN expression was expressed as fold induction of luciferase activity. Error bars represent the mean ± S.D. for triplicates. Induction of

TRIM25 after IFN treatment was shown by immunoblot (**C**). (**E**) The Huh7.25.CD81 cells were transfected for 48 hrs with 5 μg of His-Myc-Ubiquitin expression plasmid in absence or presence of a plasmid expressing HA-TRIM25 and infected with SeV (40 HAU/ml) or HCV (m.o.i = 6). At the times indicated, 10% of the lysate was precipitated with TCA and the remaining lysate subjected to nickel pulldown under denaturing conditions. Total and ubiquitin (Ub)-modified proteins were separated by SDS-PAGE and revealed by immunoblot.
doi:10.1371/journal.ppat.1002289.g001

assay (**Figure 3C**). Very limited additional effect was observed in the concomitant presence of siRNAs targeting PKR. (**Figure 3B**). Interestingly, we noticed that expression of luciferase from the IFNβ promoter increased throughout the first 18 hours of HCV infection in the siISG15 cells (**Figure 3C**). This was intriguing as it should have been inhibited after 12 hours of HCV infection through the eIF2α kinase activity of PKR and its control on translation [8]. We therefore analysed whether the state of PKR activation (phosphorylation) was dependent on the expression of ISG15. For this, the Huh7.25.CD81 cells were transfected either with siRNAs targeting ISG15 or with a plasmid expressing an HA-ISG15 construct and PKR phosphorylation was analysed as described previously [8]. The results showed that depletion of ISG15 inhibits PKR activation in the HCV-infected cells, while its overexpression stimulates it (**Figure 3D** and **Figure S5**). Therefore these data reveal that, in addition to negatively controlling RIG-I ubiquitination, ISG15 can also positively control PKR activity. The conjugation of both effects results in an efficient control of IFN induction during HCV infection.

HCV triggers a PKR-dependent pathway early in infection to induce ISG15 and other genes

The Huh7.25.CD81 cells express ISG15 at significant basal levels. This situation was not surprising as various cellular systems can also express some of the ISGs at basal level. Expression of ISG15 was approximately 2- and 5-fold higher in the Huh7.25.CD81 cells than in the Huh7.5 or Huh7 cells (data not shown). Intriguingly however, we noticed that ISG15 expression was increased in response to HCV infection (see **Figure 2E**). To investigate this further, we simply re-used the RNAs prepared for the experiment shown in Figure 3B and performed a quantitative kinetics analysis. The results confirmed that HCV can trigger induction of ISG15 (**Figure 4A**). Unexpectedly, analysis of the RNA extracted from the cells treated with siRNAs targeting PKR, revealed that ISG15 RNA expression was strongly repressed when PKR was silenced (**Figure 4A**). This surprising result was confirmed by analysing induction of ISG56, another early ISG [26], both at the level of its endogenous RNA (**Figure 4B**) or by using an ISG56-luciferase vector (**Figure 4C**). In the latter case, a strong increase of the reporter expression in the cells treated with siRNAs targeting ISG15, was similar to the situation observed for IFNβ RNA (**Figure 2B and 2C**). This can be related to activation of the RIG-I pathway, which can function when ISG15 is absent. These data suggest that HCV may use PKR to activate gene transcription. Importantly, this phenomenon was specific to HCV as infection with Sendai virus resulted in a similar induction of ISG15 and ISG56, regardless of PKR (**Figure 4D and Figure S6**). We then examined whether overexpression of PKR could boost induction of ISG15 during HCV infection and how this would affect HCV replication and IFN induction, in relation to the pro-HCV action of ISG15. Huh7.25.CD81 cells were transfected with a plasmid expressing PKR alone or in presence of siRNAs targeting ISG15, before being infected with HCV over 48 hours. Overexpression of PKR increased the ability of HCV to induce ISG15 and concomitantly, led to an increase in HCV RNA expression. The latter increase was abolished when ISG15 was silenced, thus showing that the PKR-dependent increase in HCV expression is mediated by ISG15 (Figure **4E**). However, while the cells silenced for ISG15 are able to induce IFN in response to HCV infection, as shown in Figure 3B, they are unable to do so when PKR is overexpressed. This suggests that PKR may also interfere with the process of IFN induction, independently of ISG15, a possibility that remains to be explored.

A role for PKR in gene induction in response to HCV infection has not been described before. Additional information was therefore obtained through a transcriptome analysis of 2165 genes in the Huh7.25.CD81 cells treated with control siRNAs or siRNAs targeting PKR and infected with HCV for 12 hrs. Out of the most significant 422 genes that were identified, 99 were unmodified or barely modified and 33 were down-regulated, while 290 genes were found to be up-regulated by HCV infection (data not shown). Among those, HCV infection triggered up-regulation of 49 genes which are directly dependent on PKR expression (**Table 1**). Forty percent of these genes (20) belong to the family of the ISGs, with ISG15 among the most induced genes (**Table 1**). In the reciprocal situation, only 17 genes depended on PKR for their down-regulation by HCV infection, with no link to a particular family of genes and limited variation both in number and intensity (**Table S1**). Thus, induction of ISGs upon HCV infection may occur through a novel signaling pathway that involves PKR.

Induction of ISG15 by HCV is independent of RIG-I, involves MAVS/TRAF3 association with PKR and involves the DRBD region but not the catalytic activity of PKR

Infection with RNA viruses or transient transfection with dsRNA can directly and rapidly induce early ISGs, such as ISG15, through IRF3, after activation of the RIG-I/MAVS pathway and recruitment of TRAF3, an essential adapter which recruits the downstream IRF3 kinases TBK1/IKKε. We have shown that the RIG-I pathway was not operative during HCV infection in the Huh7.25.CD81 cells, precisely due to the presence of ISG15. To determine how ISG15 induction through PKR relates to or differs from the RIG-I/MAVS pathway, the Huh7.25.CD81 cells were treated with siRNAs aimed at targeting separately PKR, RIG-I, MAVS, TRAF3 and IRF3 (**Figure S7**) and infected with HCV. The results clearly showed that induction of ISG15 in response to HCV infection depends on PKR, MAVS, TRAF3 and IRF3 but not on RIG-I (**Figure 5A**). The participation of IRF3 was further confirmed by immunofluorescence studies which showed its nuclear translocation at 6 hours post-infection (**Figure S8**). ISG15, as well as ISG56, was also clearly induced in response to HCV infection in two other HCV permissive cell lines, such as Huh7 and Huh7.5 cells, and this induction was abrogated in presence of siRNAs targeting PKR (**Figure 5B and Figure S9**). Importantly, since Huh7.5 cells express a non-functional RIG-I/MAVS pathway due to a mutation in RIG-I, result with these cells supports the notion that the ability of HCV to trigger induction of ISGs through PKR is independent of RIG-I. To have more insights on this novel PKR signaling pathway, PKR was immunoprecipitated at early times points following infection of Huh7.25.CD81 cells with HCV and the immunocomplexes were analysed for the presence of MAVS, TRAF3 and RIG-I. Both MAVS and TRAF3, but not RIG-I, associate with PKR in a time dependent manner, beginning at 2 hrs post-infection (**Figure 5C**). Strikingly, these associations were abrogated by the cell-permeable peptide PRI which is analogous to the first dsRNA binding

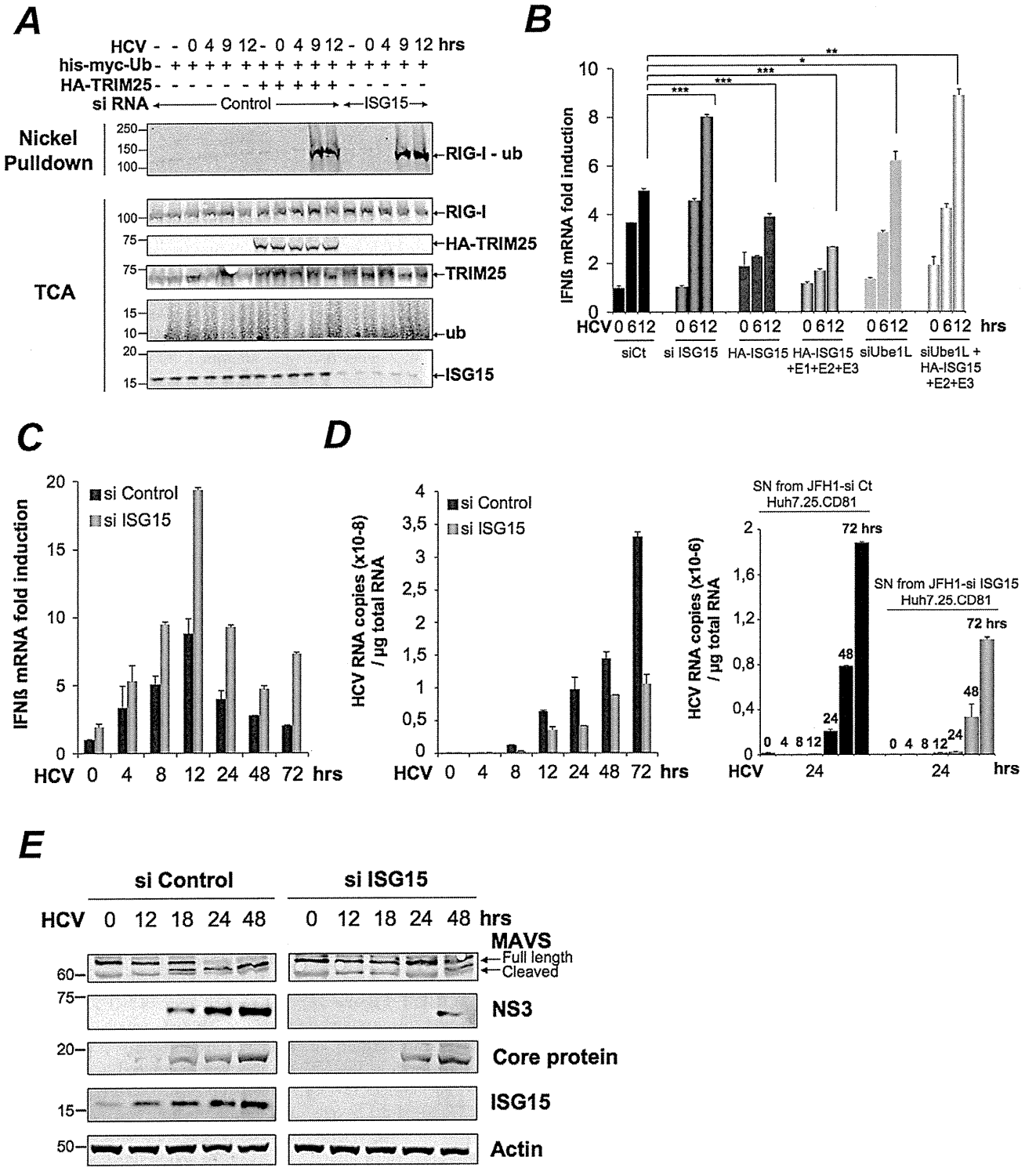

Figure 2. HCV controls RIG-I ubiquitination through ISG15. (**A**) Huh7.25.CD81 cells were transfected for 24 hrs with 25 nM of siRNA (Control or ISG15) and for another 24 hr with 5 µg of a His-Myc-Ubiquitin plasmid in absence or presence of 5 µg of a plasmid expressing HA-TRIM25. The cells were infected with JFH1 (m.o.i = 0.2). At the times indicated, cell extracts were processed for analysis of RIG-I ubiquitination and the expression of the different proteins in the total cell extracts. (**B**) Huh7.25.CD81 cells were first transfected with siRNA Control (25 nM), si RNA ISG15 (25 nM), siRNA Ube1L (50 nM) or left untreated. After 24 hrs, the untreated cells were transfected with a plasmid expressing HA-ISG15 (500 ng) alone or in presence of plasmids expressing E1, E2 and E3 (1 µg each) while a set of cells transfected with siRNA Ube1L received plasmids expressing HA-ISG15, E2 and E3. After 24 hrs, the cells were infected with JFH1 (m.o.i = 6) for the times indicated. Stimulation of endogenous IFNβ RNA expression was determined by RTqPCR and expressed as fold induction. The degree of statistical significance is indicated by stars after calculation of the p-values (from left to right: 0.0005, 0.0076, 0.0003, 0.047 and 0.0023). (**C–D**) Huh7.25.CD81 cells, transfected with 25 nM of siRNA (Control or ISG15) for 48 hrs, were infected with JFH1 (m.o.i = 6) for the times indicated. Expression of IFNβ or HCV RNA, determined by RTqPCR, was expressed as fold induction (**C**; IFNβ) or as copies (**D**; HCV). Error bars represent the mean ±S.D for triplicates. Expression levels of IFNβ RNA at the start of infection were 2.1×10^4 (siControl) and 4×10^4

copies (siISG15). Supernatants collected at different times post-infection were used to infect fresh cells. After 24 hours, the RNAs were extracted from the cells and expression of HCV RNA was determined by RTqPCR. (**E**) Huh7.25.CD81 cells, transfected with 25 nM of siRNA (Control or ISG15) for 48 hrs, were infected with JFH1 for the times indicated. Cell extracts were analysed by immunoblot with Abs directed against ISG15, MAVS, the HCV NS3 and core proteins and Actin as loading control.
doi:10.1371/journal.ppat.1002289.g002

domain (DRBD) of PKR [8], while unaffected by C16, a chemical compound which inhibits the catalytic activity of PKR (**Figure 5D**). In line with this, PRI but not C16, abrogated the ability of HCV to induce ISG15 (**Figure 5E**). The same result was obtained for induction of ISG56 (**Figure S10**). We then used human primary hepatocytes (HHP) to determine whether HCV was also able to induce ISGs through PKR in a more physiological cellular model. A follow-up of the infection over a period of 96 hours showed that JFH1 was replicating correctly in those cells as well as leading to induction of ISG15 (10-fold) and to some induction of IFNβ (2.5-fold). These cells were infected with JFH1 for 8 hours in the absence or presence of PRI, making convenient

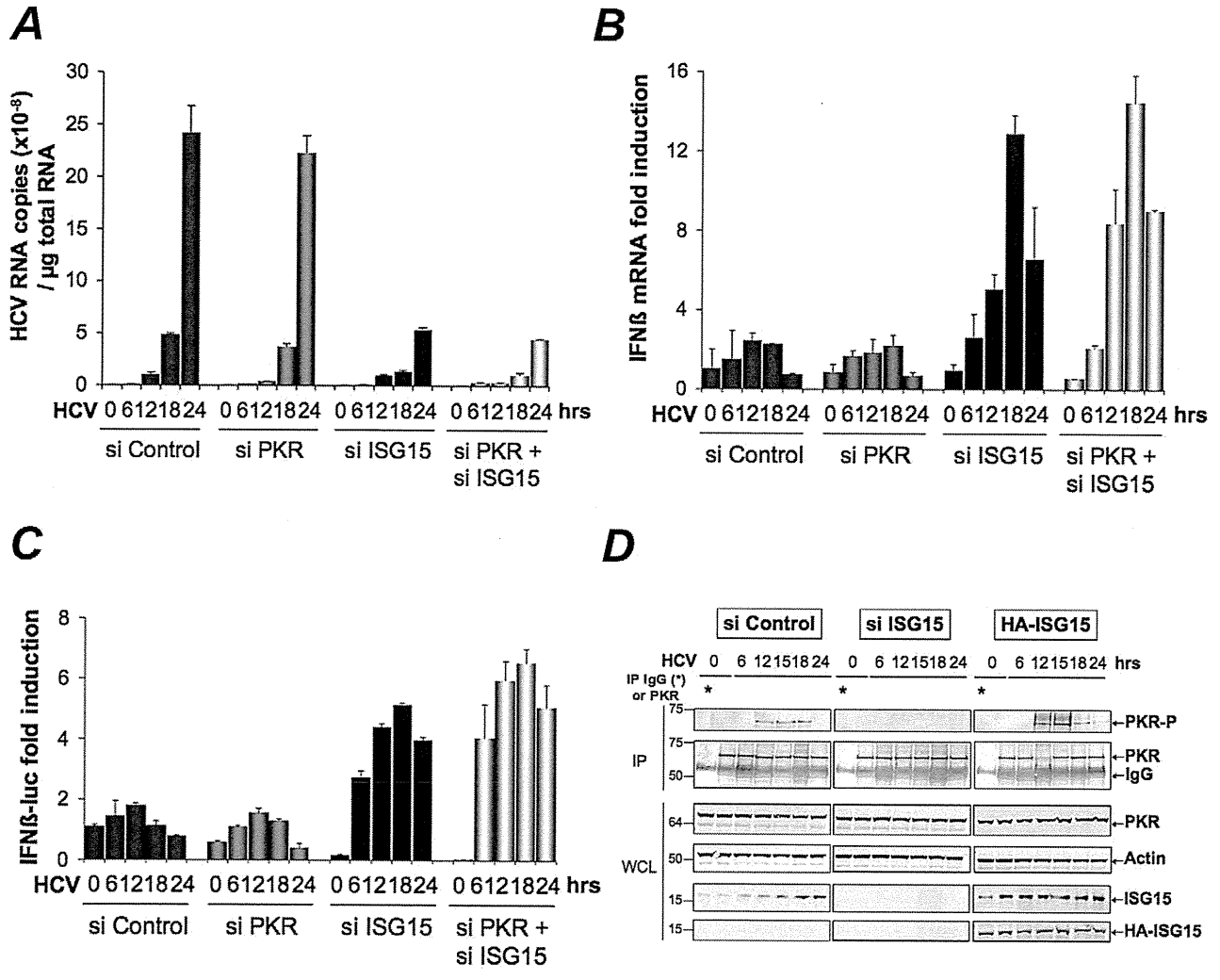

Figure 3. ISG15 strengthens the pro-HCV activity of PKR. (**A–B**). The Huh7.25.CD81 cells were transfected with 25 nM of the different siRNA (Control, ISG15, PKR), separately or together. After 48 hrs, cells were infected with JFH1 (m.o.i = 0.2). At the times indicated, expression of HCV or IFNβ RNA was determined by RTqPCR and expressed as copies of JFH1 RNA (**A**) or as fold induction (IFNβ; **B**). The expression levels of IFNβ RNA at the start of infection was 6.96×10^5 copies. (**C**) Two sets of Huh7.25.CD81 cells were first transfected with siRNA ISG15, siRNA PKR separately and together for 24 hrs, then transfected with the reporter plasmids IFNβ-firefly luciferase (pGL2-IFNβ), pRL-TK Renilla-luciferase for another 24 hrs and infected with JFH1 (m.o.i = 0.2) for the times indicated. In each case, IFN expression was expressed as fold-induction over control cells that were simply transfected with pGL2-IFNβ-FLUC/pRL-TK-RLUC. The graph represents the level of firefly luciferase activity normalized to the ratio R-luc RNA/GAPDH RNA. Such normalization is required because of the negative control of general translation through PKR after 12 hrs post-infection [8]. Error bars represent the mean ±S.D for triplicates. (**D**) Huh7.25.CD81 cells, in 100 cm^2 plates, were transfected with siRNA Control or siRNA ISG15 or transfected with a plasmid expressing HA-ISG15 for 48 hrs and infected with JFH1 (m.o.i = 6). At the indicated times post-infection, cell extracts (2.2 mg) were processed for immunoprecipitation of PKR or for incubation with mouse IgG as a control of specificity (asterisk). The immunoprecipitated complexes were run on two different NuPAGE gels and blotted using Mab 71/10 or anti-phosphorylated PKR antibodies (PKR-P). The presence of PKR and PKR-P was revealed using the Odyssey procedure. The ratio PKR-P/PKR in the absence or in the presence of ISG15, either endogenous or endogenous and ectopic, is shown in Figure S5.
doi:10.1371/journal.ppat.1002289.g003